



**NUST COLLEGE OF
ELECTRICAL & MECHANICAL
ENGINEERING**

**ANALYSIS AND DEVELOPMENT OF NOVEL
INSULATOR FOR HIGH VOLTAGE TRANSMISSION
LINES**

FINAL YEAR PROJECT REPORT

DE-41 (DME)

Submitted by

RANA MUNEEB ANEES

BILAL AHMED

BACHELORS IN

MECHANICAL ENGINEERING

YEAR

2023

PROJECT SUPERVISOR

DR. IMRAN AKHTAR

**NUST COLLEGE OF
ELECTRICAL AND MECHANICAL ENGINEERING
PESHAWAR ROAD, RAWALPINDI**

DECLARATION

We hereby declare that no portion of the work referred to in this Project Thesis has been submitted in support of an application for another degree or qualification of this or any other university or other institute of learning. If any act of plagiarism is found, we are fully responsible for every disciplinary action taken against us depending upon the seriousness of the proven offence, even the cancellation of our degree.

COPYRIGHT STATEMENT

- Copyright in text of this thesis rests with the student author. Copies (by any process) either in full, or of extracts, may be made only in accordance with instructions given by the author and lodged in the Library of NUST College of E&ME. Details may be obtained by the Librarian.
- This page must form part of any such copies made. Further copies (by any process) of copies made in accordance with such instructions may not be made without the permission (in writing) of the author.
- The ownership of any intellectual property rights which may be described in this thesis is vested in NUST College of E&ME, subject to any prior agreement to the contrary, and may not be made available for use by third parties without the written permission of the College of E&ME, which will prescribe the terms and conditions of any such agreement.
- Further information on the conditions under which disclosures and exploitation may take place is available from the Library of NUST College of E&ME, Rawalpindi.

ACKNOWLEDGEMENTS

Alhumdulillah, WE MADE IT.

Thank you to ALLAH ALMIGHTY, for His countless blessings and guidance which helped us complete our degree with our heads held high. We would like to extend our sincere appreciation to Dr. Imran Akhtar for his invaluable supervision, guidance, and encouragement throughout our project. His expertise, wisdom, and unwavering support have been instrumental in shaping our research and achieving our goals. Thank you to the group for always pulling through and sticking together. We would like to acknowledge the assistance and cooperation received from the faculty and staff of the Department of Mechanical Engineering for supporting us through the 4 years of our tenure here at C of EME, NUST. Their provision of necessary resources, access to facilities, and academic support have greatly facilitated our research process. And finally Thank you to our families and friends who prayed for us and kept us going with their kind acts and words.

ABSTRACT

Porcelain insulators play a critical role in ensuring the reliable transmission of electrical power in overhead power lines. They provide essential insulation against high voltages, effectively preventing electrical leakage and ensuring the safe and efficient flow of electricity. However, predicting the useful serviceable life of porcelain insulators is a challenging task, often requiring periodic verification to maintain their reliability. One of the primary concerns associated with porcelain insulators is the accumulation of salt and dust particles on their surface. Over time, these contaminants reduce the efficiency of the insulators, increasing the risk of flashovers. Flashovers, caused by the electrical discharge across insulator surfaces, disrupt the smooth power evacuation process, leading to power outages and compromising the overall efficiency of the transmission system. To address this issue, we propose the development of an innovative solution—an insulator that is capable of self-cleaning through the action of wind. By utilizing the natural force of wind, the insulator's surface would be continuously cleaned, preventing the accumulation of salt and dust particles. This automated cleaning process would significantly reduce contamination, minimizing the risk of flashovers and ensuring the uninterrupted flow of electricity. Implementing such a self-cleaning insulator would bring numerous benefits. Firstly, it would eliminate the need for time-consuming and costly manual cleaning processes, reducing maintenance efforts and associated expenses. Moreover, this solution would enhance worker safety by eliminating the requirement for hazardous cleaning procedures. Additionally, the improved cleanliness of the insulators would lead to a reduction in power outages, enhancing the reliability and efficiency of power transmission systems.

TABLE OF CONTENTS

Declaration.....	1
Copyright Statement.....	2
Acknowledgements.....	3
Abstract.....	4
Table of Contents.....	5
List of Tables.....	8
List of Figures.....	9
List of Symbols.....	11

Chapter 1

Introduction

1.1 Motivation.....	12
1.2 Literature Review.....	13
1.2.1 Porcelain Insulator	13
1.2.2 Spiral Insulator.....	13
1.3 Insulator Properties	14
1.4 Insulator Material.....	15
1.5 Types of Insulators.....	15
1.5.1 Pin Type Insulators	15
1.5.2 Suspension Insulators.....	16
1.5.3 Shackle Insulators	16
1.6 Advantages of Porcelain Insulators	17
1.7 Insulation Failure	18
1.8 Conventional Insulator.....	19
1.9 Problem Identification	20
1.10 SDGs.....	20

1.11 Market Research	21
1.12 Engagement with Industry	22
1.13 Ease of Adoption.....	23

Chapter 2

Geometry and Mesh

2.1 CAD Models	24
2.1.1 Novel Design 1	24
2.1.2 Novel Design 2	25
2.1.3 WAPDA Requirements.....	26
2.2 Meshing.....	26
2.2.1 Mesh for Conventional Design	27
2.2.2 Mesh for Novel Design 1	29
2.2.3 Mesh for Novel Design 2.....	30
2.2.4 Mesh Independence Test.....	31

Chapter 3

Numerical Methodology

3.1 Governing Equations	33
3.1.1 Continuity Equation	33
3.1.2 Momentum Equation	34
3.2 Turbulence Modelling.....	34
3.2.1 k- ω SST Turbulence Model	34
3.2.2 SIMPLE Algorithm.....	35
3.3 Boundary Conditions	36
3.3.1 Velocity Inlet	36

3.3.2 Pressure Outlet	37
3.3.3 Insulator Walls	37
3.4 Solver Setup	38

Chapter 4

Physical Testing

4.1 Development of Prototypes.....	39
4.2 Experimental Setup.....	41
4.3 Experimental Procedure.....	42
4.4 Experimental Results	43

Chapter 5

Results and Discussion

5.1 Contours of Pressure Magnitude.....	47
5.2 Contours of Velocity Magnitude	49
5.3 Pressure and Velocity Variation Before and After Geometry	51
5.4 Distribution of Pressure Along Geometry	54
5.5 Validation.....	56

Chapter 6

Conclusion.....	57
-----------------	----

Chapter 7

Limitations.....	58
------------------	----

Chapter 8

Future Recommendations.....	59
-----------------------------	----

References:	61
--------------------------	----

LIST OF TABLES

Table 2.1 Creep distance.....	26
Table 2.2 Mesh independence	31
Table 3.1 Solver setup	38
Table 4.1 Dead weights of insulators	43
Table 4.2 Comparison 1	44
Table 4.3 Comparison 2	44
Table 5.1 Pressure and velocity difference	54

LIST OF FIGURES

Figure 1.1 Pin insulator	15
Figure 1.2 Suspension insulator.....	16
Figure 1.3 Shackle insulator.....	17
Figure 1.4 Conventional design	19
Figure 1.5 EM-369MK.....	21
Figure 1.6 EM-507.....	22
Figure 1.7 EM-5K.....	22
Figure 2.1 Fermat spiral applied to EM-369MK	24
Figure 2.2 Spiral applied to EM-369MK.....	25
Figure 2.3 Mesh for geometry and bounding box.....	28
Figure 2.4 Mesh around insulator	28
Figure 2.5 Mesh for geometry and bounding box.....	29
Figure 2.6 Mesh around insulator	29
Figure 2.7 Mesh for geometry and bounding box.....	30
Figure 2.8 Mesh around insulator	30
Figure 2.9 Mesh independence test	32
Figure 4.1 Prototype 1 (conventional design)	39
Figure 4.2 Prototype 2 (novel design 1)	40
Figure 4.3 Prototype 3 (novel design 2)	40
Figure 4.4 Experimental setup	42
Figure 4.5 Deposits on conventional design.....	45
Figure 4.6 Deposits on novel design 1	46
Figure 4.7 Deposits on novel design 2.....	46
Figure 5.1 Pressure contours on conventional design	48
Figure 5.2 Pressure contours on novel design 1	48
Figure 5.3 Pressure contours on novel design 2.....	49
Figure 5.4 Velocity contours on conventional design	50
Figure 5.5 Velocity contours on novel design 1	50

Figure 5.6 Velocity contours on novel design 2.....51
Figure 5.7 Pressure variation along conventional insulator.....52
Figure 5.8 Velocity variation along conventional insulator.....53
Figure 5.9 Pressure variation along novel design 2.....53
Figure 5.10 Velocity variation along novel design 254
Figure 5.11 Pressure distribution along conventional design path55
Figure 5.12 Pressure distribution along novel design 2 path55
Figure 5.13 Validation.....56

LIST OF SYMBOLS

- r Distance from the origin (the center of the spiral) to a point on the spiral
- t Angle between the radial line from the origin to the point and a fixed reference line
- a Scaling factor
- ρ Density
- u Velocity
- Re Reynolds number
- k Turbulent kinetic energy
- ρk Turbulence production term
- Pr Prandtl number
- β Coefficient for turbulent Prandtl number
- ω Specific dissipation rate
- μ Dynamic viscosity
- μ_t Turbulent viscosity
- σ_k Turbulent Prandtl number for k
- Gk Generation of turbulent kinetic energy due to mean velocity gradients

Chapter 1

Introduction

Porcelain insulators (bell type) were first created in 1849 by Werner von Siemens. Porcelain insulators were originally used for insulation of telephone lines. Since then, porcelain insulators have evolved and have found vast usage especially in the transmission lines system acting as insulators.

Porcelain insulators have two basic purposes on transmission lines:

- To support conductors and attach them to structures.
- To electrically isolate conductors from other components on a transmission line.

The second purpose is very important to operation since without some form of insulating material, electrical circuit cannot operate.

To be able to isolate conductors, insulators must be made of materials that offer a great deal of resistance to the flow of electricity. Porcelain is one of the most highly used insulator types along with glass and other synthetic materials. Porcelain is a multiphase ceramic material that is obtained by heating aluminum silicates until a mullite phase is formed. Mullite is porous, its surface must be glazed with a high melting point glass to render its smooth and impervious for use in overhead line insulators. Porcelain insulators, like any insulators, come in a variety of different shapes and sizes, to accommodate the insulator rating as well as its usage. Insulators are rated in terms of their electrical and mechanical handling capabilities.

1.1 Motivation

National Transmission & Dispatch Company (NTDC) transmits electricity through 5770 km of 500 KV and 9700 km of 220 KV transmission lines. Tripping of NTDC network caused a non-delivery of 1.9 billion units (kWh) during the season of high fog/smog and high humidity causing a financial loss of Rs. 226 million in respect of wheeling charges (Jan 2018 to Jan 2019). Most of the tripping issues occur due to pollution contamination and moisture, forming

a conductive layer on disc insulators leading to flashover especially in coastal and industrial areas. The tripping issue in NTDC due to flashover is a leading cause of severe local and partial outages of power supply to the end consumers.

Keeping all these points in mind we find it motivating to be able to design and develop a novel insulator that will mitigate contamination deposits and reduce flashover using aerodynamics as a passive control.

Novel insulator design find its application natural to power distribution systems. The novel insulator design will minimize the contamination deposit, reduce the cleaning cost, and save the national exchequer.

1.2 Literature Review

1.2.1 Porcelain Insulator

The consumption of electric energy has been significantly increasing in developing countries due to the rapid evolution of industries and changes in human lifestyle. For instance, in Ethiopia the energy sector has been growing in the past two decades and reached currently electric power of 2360 MW, this would be expected to reach 10,000 MW in the next 10 years [1]. Hence, the power industries work all the way to develop high voltage and long-distance transmission. For safe transmission and distribution of the electric power, application of insulator is very much essential to prevent the flow of current from the wire to the earth through ground supporting tower or poles.

Among the insulator materials utilized in electric power transmission and distribution system porcelain insulator is the most used material for overhead insulators. Porcelain insulators were found to exhibit excellent properties such as high mechanical strength, high electrical stability, and corrosive resistance even in humid environments [2]. Moreover, the raw materials used for its production are also naturally available compared to other types of insulators which need industrially processed materials [3].

1.2.2 Spiral Insulator

The novel spiral design incorporated in the insulator structure, inspired by the abundant presence of spiral patterns in nature, offers a unique and effective solution to combat dust deposition. Natural spirals, observed in phenomena such as galaxies, seashells, and plants, have

served as valuable inspiration for our team in developing innovative engineering solutions. By introducing a spiral path on the insulator surface, we disrupt the smooth airflow, inducing turbulence that prevents the settling of dust particles. This novel design not only enhances self-cleaning capabilities but also improves insulation performance.

Beyond high voltage transmission line insulators, the spiral design concept holds potential for applications in various fields. In air filtration systems, the turbulence generated by the spiral configuration can prevent clogging and enhance the efficiency and lifespan of filters in HVAC systems, industrial settings, and cleanrooms. Additionally, the spiral design can be incorporated into building materials or coatings, enabling self-cleaning surfaces that utilize the natural flow of air or water to dislodge and remove debris, reducing the need for manual cleaning and maintenance.

Furthermore, the spiral design concept may find use in fluid dynamics and heat transfer systems. By incorporating spirals into heat exchangers or flow channels, the enhanced turbulence improves heat transfer efficiency and prevents fouling or scaling, leading to more efficient and reliable thermal management.

While further research and development are required, the versatile nature of the spiral design offers opportunities for implementation in fields where dust deposition, filtration, or self-cleaning functionalities are crucial.

1.3 Insulator Properties

Insulators have some specific properties that make them different from other electrical devices [4]. These are some features of insulators:

- High mechanical strength and durability.
- Excellent electrical insulation properties.
- Good resistance to thermal and electrical shocks.
- Resistance to weathering and aging.
- Low thermal expansion coefficient.
- High melting point and chemical stability.
- Non-porous surface that prevents the accumulation of pollutants.
- Low maintenance requirements.
- Easy to clean and maintain.

- High resistance to vandalism and wildlife interference.

1.4 Insulator Material

Insulators consist of different types of insulator materials like plastic, rubber, mica, wood, glass, etc. In the electrical system, specific insulating materials are used like porcelain, glass, steatite, polymer, ceramic, PVC.

1.5 Types of Insulators

For the successful operation of power lines, proper selection of insulators is essential [5]. There are several types of overhead line insulators. Most used types are:

- Pin type insulators
- Suspension type insulators
- Shackle insulators

1.5.1 Pin Type Insulators

Pin type insulators or pin insulators are popularly used in electric distribution systems up to 33 kV voltage level. They are secured on the cross arms of the pole to carry power lines [6]. There is a groove on the upper end of a pin insulator for housing the conductor. Conductor wire is passed through this groove and secured by binding with the same wire as of conductor.



Fig 1.1: Pin insulator

A pin insulator is usually made from porcelain, but glass or plastic may also be used in some cases. As pin insulators are almost always employed in the open air, proper insulation while

raining is also an important consideration. A wet pin insulator may provide a path for current to flow towards the pole. To overcome this problem, pin insulators are designed with rain sheds or petticoats. Beyond operating voltage of 33kV, pin insulators become too bulky and uneconomical.

1.5.2 Suspension Insulators

As mentioned above, pin insulators become too bulky and uneconomical beyond 33 kV. So, for voltages higher than 33 kV, suspension insulators are used. A suspension insulator consists of several porcelain discs connected to each other with metal links in the form of a string. The line conductor is suspended at the bottom end of the suspension string which is secured to cross-arm of the tower [7]. Each disc in a suspension insulator string is designed for a low voltage, say 11 kV. The number of discs in a string depends on the working voltage.



Fig 1.2: Suspension insulator

1.5.3 Shackle Insulators

Shackle insulators are used in low voltage distribution lines as strain insulators. A shackle insulator can be used vertically as well as horizontally and it can be directly fixed to a pole with a bolt or to the cross arm. However, the use of such insulators is decreasing after increasing the use of underground cables for distribution purposes



Fig 1.3: Shackle insulator

1.6 Advantages of Porcelain Insulators

- At its disposal, the porcelain insulator is not dangerous waste.
- It is manufactured from natural materials by simple blending and curing; it may be stored in dumps with other waste. It may serve as a recycled material to produce ceramic and similar products [8].
- In comparison to the polymer, the electrical strength of porcelain is higher. The porcelain insulator in the dry state as electric insulation material has better electrical properties than the polymer, type electrical tests show better results, giving longer useful life in terms of loads generated by electric charges and other temporary electrical phenomena.
- It has demonstrably higher resistance to degradation of the surface, does not degrade or carbonate during charges; the conductive path is created very slowly in comparison to the surface of a composite-material insulator.
- High thermal resistance and strength because ceramics are resistant to temperatures as high as 1000°C.
- Porcelain material is resistant to rodents, termites, birds, and other animals capable of compromising the integrity of polymers.
- The features of high plasticity during production, the possibilities of precision grinding and quite easy cementation and bonding with excellent mechanical properties permit that a multitude of shapes be created and used in any type of application.

- It is suitable for extreme hot/cold changes in the environment. It is suitable for environments with dust, salt, and high moisture, or for combination of all the above.
- The highly glazed surface gives the product better self-cleaning properties in high-pollution areas. The product shows stable results in charges and short-circuit in this type of environment; it is highly resistant to corrosion in acidic as well as caustic environments.
- It does not suffer from defects in the ceramics-to-metal interface.
- The combination of the porcelain insulator with cast-iron or aluminum structures using traditional cementing agents is resistant to transition phenomena during the discharge or brush discharge.
- It offers very high mechanical strength under pressure and hardness. It does not deform unless external force is deployed. Long useful life can be guaranteed of lengths up to 40 years. Therefore, many users have provided long-term operational references in several applications.
- The design is modified to suit the environment. The product offers many shapes during production; glazing uses a wide scale of colors based on the needs of the customer, for example grey or sky blue.
- They can be combined with cast-iron or aluminum structures using traditional cementing agents, resisting transition phenomena during discharge.
- Porcelain insulators have high mechanical strength, hardness, and dimensional stability, guaranteeing a long useful life.
- The design of porcelain insulators can be modified to suit specific environments, and a wide range of colors are available for glazing options, catering to customer preferences.

1.7 Insulation Failure

An insulator must be properly designed to withstand mechanical as well as electrical stresses. Electrical stress on insulator depends on the line voltage, and hence, proper insulators must be used according to the line voltage. Excess electrical stress can break down the insulator either by flash-over or puncture.

- **Flash-over:** In insulator flash-over, electrical discharge occurs by forming an arc between the line conductor and the insulator pin (which is connected to the cross-arm). The discharge jumps through the air surrounding the insulator following the shortest distance [9]. In case of a flash-over, the insulator continues to act according to its designed capacity unless it gets destroyed due to the excess heat.
- **Puncture:** In case of insulator puncture, electrical discharge occurs from conductor to pin through the body of the insulator. Sufficient thickness of porcelain (or the insulator material) must be provided to avoid a puncture breakdown. When such a breakdown is involved, the insulator is permanently damaged.

1.8 Conventional Insulator

A conventional insulator design comprises concentric circles and are prone to trapping contamination and moisture due to stagnations points. It requires regular cleaning to remove dust, soot, and other contaminations causing effort and cost.

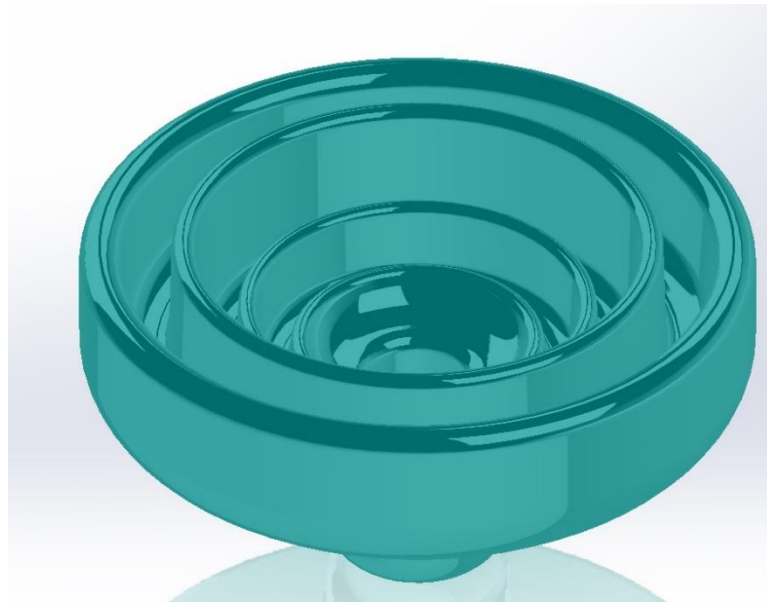


Fig 1.4: Conventional design

1.9 Problem Identification

The environment is contaminated with dust particles and these dust particles are more electrically conductive than insulator material. Dust particles flow with air as the wind blows and are deposited on the insulator surface. Dust particles decrease efficiency of insulators by increasing electrical conductivity which leads to electrical arcing and flashovers [10].

Flashover on a disruptive electrical discharge over the surface of solid insulation is caused by the high conductivity when it becomes wet (e.g., from light rain conditions such as dew, fog, light rain, etc.).

The arcing leads to short circuiting causing very serious injuries to the maintenance crew. Short circuiting also leads to city wide electricity breakdowns causing difficulties for the city population and industries. Safety hazards and electricity breakdowns result in bad PR for the company resulting in low employee morale, voluntary turnover, and a decline in sales.

1.10 SDGs

SDG 7: Affordable and Clean Energy

Novel insulator contributes to SDG 7 by promoting the generation and transmission of affordable, reliable, and clean energy. By improving the efficiency and reliability of high voltage transmission lines through the novel insulator, we enable the smooth transmission of electricity from renewable energy sources such as wind and solar power. This aligns with the goal of ensuring access to affordable, reliable, sustainable, and modern energy for all, while also supporting the reduction of greenhouse gas emissions and the transition to a more sustainable energy system.

SDG 9: Industry, Innovation, and Infrastructure

The novel insulator aligns with SDG 9 by promoting sustainable industrialization, fostering innovation, and building resilient infrastructure. Through our efforts to enhance the performance and reliability of insulators for high voltage transmission lines, we contribute to the development of sustainable infrastructure for energy transmission. By integrating innovative materials and designs into the insulator, we demonstrate our commitment to

technological advancements that drive sustainable development. This supports the goal of building resilient infrastructure and promoting sustainable industrialization.

SDG 11: Sustainable Cities and Communities

Our novel insulator for high voltage transmission lines directly contributes to SDG 11 by promoting sustainable cities and communities. Reliable electricity transmission is a fundamental requirement for urban areas, ensuring a stable and uninterrupted power supply for homes, businesses, and public services. By enhancing the efficiency and resilience of high voltage transmission lines through our insulator, we enable the development of sustainable, inclusive, and resilient cities. This critical infrastructure component supports the establishment of smart grids, facilitates the integration of renewable energy sources, and helps reduce energy losses during transmission.

1.11 Market Research

The insulator market is currently served by manufacturers such as Highland Ceramics, Versatile Business Ltd, and EMCO Industries. These manufacturers play a significant role in meeting the demand for insulators in various industries. They are known for their expertise in producing high-quality insulators and have established a strong reputation in the market. Our project aims to introduce a novel insulator design that will contribute to this competitive market by providing innovative and efficient solutions.

Some of the insulators currently available in the market are given below:

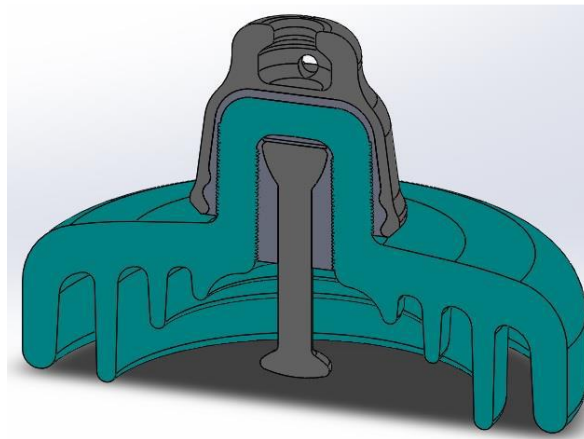


Fig 1.5: EM-369MK

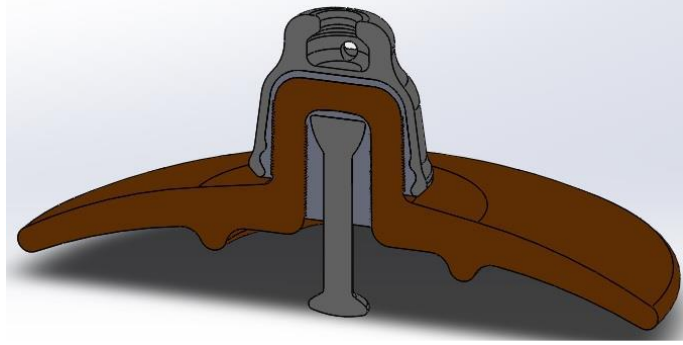


Fig 1.6: EM-507

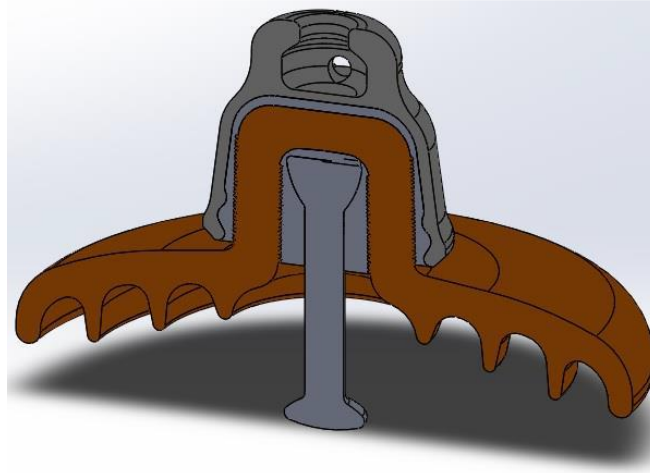


Fig 1.7: EM-5K

1.12 Engagement with Industry

Industry support and engagement are crucial for the successful manufacturing of our novel design for high voltage transmission lines. Collaborating with industry partners will grant us access to specialized facilities and resources necessary for large-scale production while meeting industry standards. By working closely with industry experts, we can optimize production techniques, ensuring efficient and cost-effective manufacturing. Industry collaboration also provides valuable market insights, allowing us to refine our design based on market demands, increasing its commercial viability. Furthermore, industry support facilitates

technology transfer and commercialization, enabling us to bring our design to market and contribute to the advancement of high voltage transmission technology.

1.13 Ease of Adoption:

- Our product boasts improved efficiency, providing better performance than traditional options.
- Additionally, our product has a longer lifespan than conventional insulators, resulting in cost savings over time.
- Our insulator also possesses environment-friendly characteristics, making it a sustainable option for customers.
- With a similar installation procedure to traditional insulators, mass deployment of our product is possible.
- Customers do not require any specific product training, as our insulator is easy to use and understand.
- While the manufacturing cost of our insulator is almost comparable to conventional insulators, the running cost is significantly lower.
- Cost savings and ease of use makes our novel insulator a beneficial choice for customers to adopt.

Chapter 2

Geometry and Mesh

2.1 CAD Models

2.1.1 Novel Design 1

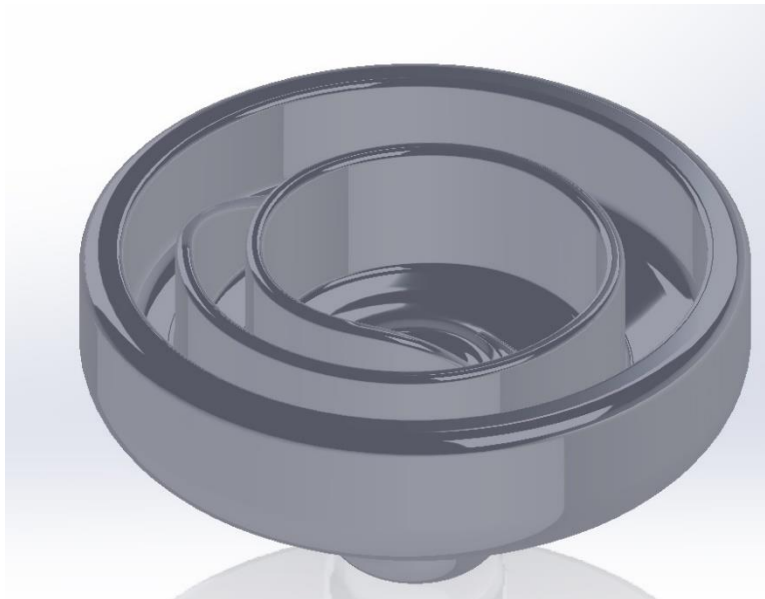


Fig 2.1: Fermat spiral applied to EM-369MK

About Fermat Spiral:

It is a mathematical concept named after French mathematician Pierre de Fermat [11]. The Fermat spiral is a geometrical figure that consists of a series of equally spaced points arranged in a spiral shape, with each point being equidistant from two fixed points (known as foci).

Fermat spiral is related to the mathematical concept of conic sections, which are shapes that are formed by intersecting a cone with a plane. In particular, the Fermat spiral is a special case of a logarithmic spiral, which is a type of spiral that appears in many natural and man-made objects, such as seashells, galaxies, and whirlpools.

The Fermat spiral has several interesting properties and applications in mathematics and physics, such as in the study of electromagnetic fields, optics, and number theory. It is also sometimes used as a design element in art and architecture.

$$t = 0: \frac{2\pi}{5} : 11.5\pi \quad (1)$$

$$r = -a \cdot (t^{1/2}) \quad (2)$$

Equations 1-2 were used in the design process of the insulator. The equation of the Fermat spiral is given by:

$$r = a\sqrt{t} \quad (3)$$

where r is the distance from the origin (the center of the spiral) to a point on the spiral, t is the angle between the radial line from the origin to the point and a fixed reference line, and a is a scaling factor that determines the size of the spiral.

This equation is often written in polar coordinates, where r is the radial coordinate and t is the angular coordinate.

2.1.2 Novel Design 2:



Fig 2.2: Spiral applied to EM-369MK

About spiral:

The original design, which had concentric circles, was modified using various commands in SolidWorks. Circular plates were removed, and the remaining sketch was refined by deleting

a quarter of it and joining the sections with tangential arcs. The sketch was then extruded to create a 3D model of the insulator. To prevent sharp edges at the start of the spiral section, a command called cut loft was used. Finally, fillets were applied to make the design smoother. This new design process improves the performance of the insulator and could be considered for future advancements in high voltage transmission systems.

2.1.3 WAPDA Requirements:

During the development of our novel insulator for high voltage transmission lines, we faced a significant challenge regarding the creep distance requirement specified by WAPDA (Water and Power Development Authority). Our initial design did not meet the specified creep distance, leading us to revise and develop a new design that aligned with WAPDA's requirements. Through careful analysis and design iterations, we successfully developed a revised design that satisfied the creep distance requirement. This experience highlighted the importance of considering and meeting regulatory standards in the development of high voltage transmission line components, reinforcing our commitment to ensuring safety and reliability in the power infrastructure.

Table 2.1: Creep distances

Property	Conventional Design	Novel Design 1	Novel Design 2
Creep Distance [m]	0.318	0.252	0.368

2.2 Meshing

The meshing of the insulator plays a crucial role in accurately analyzing and understanding its behavior and performance. In this study, after completing the modeling phase, the insulator was meshed using Ansys Mesher, employing a comprehensive meshing strategy.

The meshing process began with the implementation of the patch conforming method using tetrahedral elements. This method was chosen to ensure a precise representation of the complex

geometry and intricate details of the insulator surface. By conforming closely to the insulator's shape, this approach facilitated a more accurate analysis of its performance.

To control the element size within the volume of the insulator, body sizing was applied. Specifically, the "body of influence" type was selected, which adjusted the element size based on the proximity to specific features or regions of interest. This enabled the generation of a refined mesh, particularly in critical areas, while maintaining an appropriate element size throughout the insulator volume.

In addition to body sizing, face sizing was utilized to regulate the element size on the insulator's surface. By specifying the desired face sizing, the mesh resolution was optimized, capturing the fine features and details that significantly influence the insulator's behavior.

To accurately capture the flow behavior near the insulator, an inflation layer was added to its surface. The inflation consisted of five layers, with a first layer height thickness of 0.00035 m. This technique effectively resolved the boundary layer and enabled a more precise representation of flow gradients and boundary effects, which are vital for understanding the insulator's performance under high voltage conditions.

It is worth noting that initially, a general body sizing of 0.026 m and a face sizing of 0.0026 m were assigned to all the insulators. However, these initial sizes were refined iteratively to achieve improved results and a finer mesh. This iterative refinement process ensured that the mesh accurately captured the important features and characteristics of the insulator, enhancing the accuracy of subsequent analyses.

2.2.1 Mesh for Conventional Design:

The resulting mesh for conventional insulator consisted of 496769 nodes and 1754681 elements, ensuring a detailed representation of the insulator's features, and capturing the flow behavior near its surface.

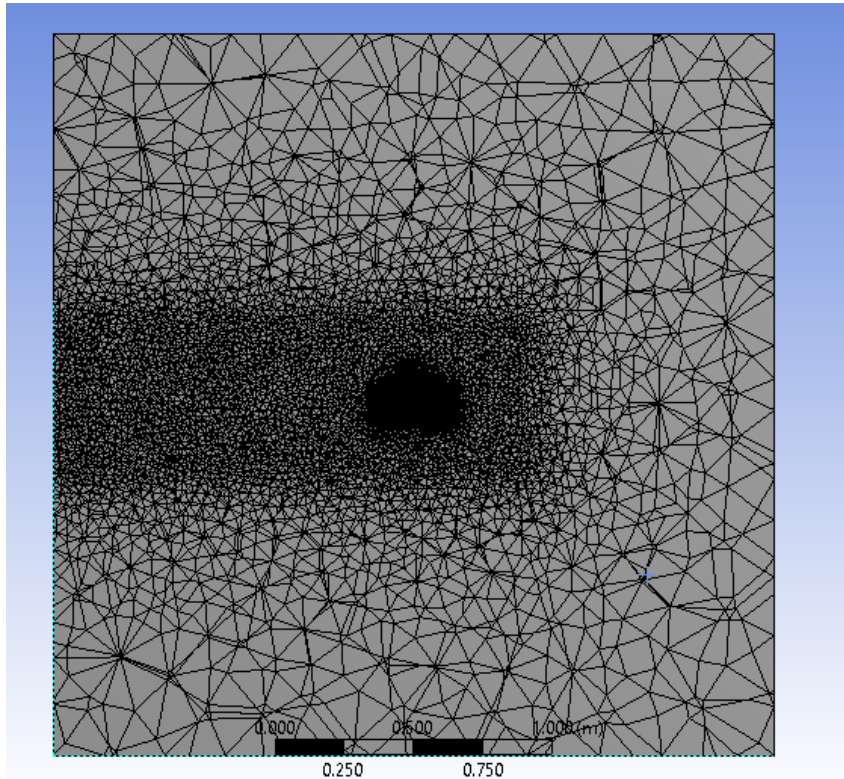


Fig 2.3: Mesh for geometry and bounding box

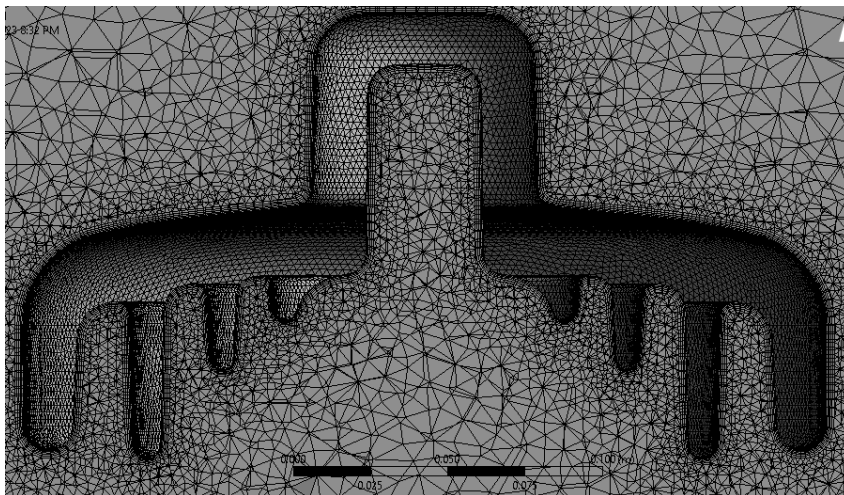


Fig 2.4: Mesh around insulator

2.2.2 Mesh for Novel Design 1:

The mesh for this insulator comprised 453425 nodes and 1643686 elements, providing a thorough representation of the insulator's geometry and accurately resolving the flow characteristics near its surface.

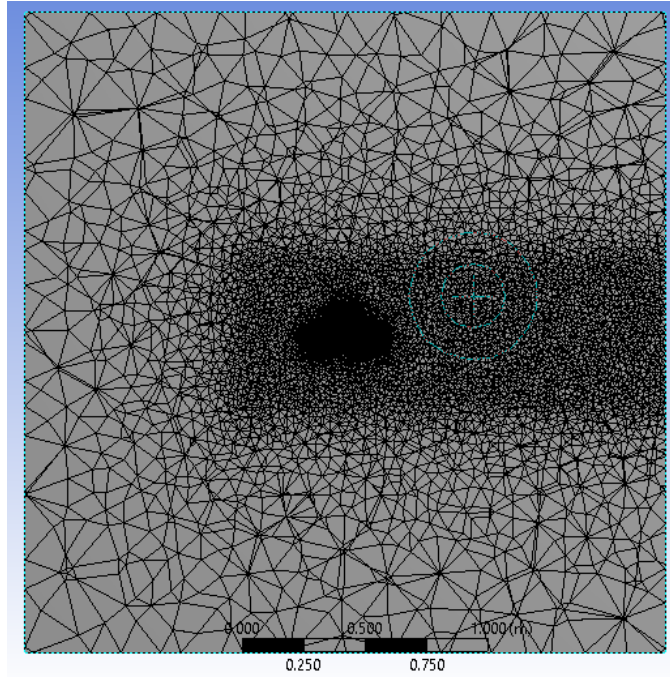


Fig 2.5: Mesh for geometry and bounding box

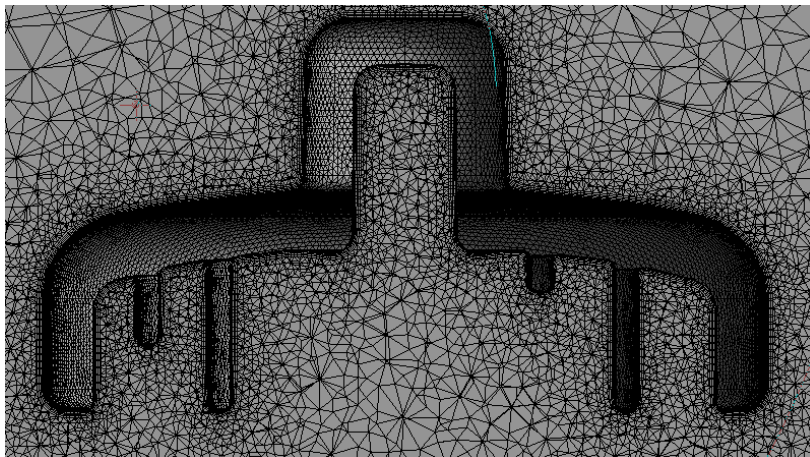


Fig 2.6: Mesh around insulator

2.2.3 Mesh for Novel Design 2:

Similarly, the mesh for this insulator was designed to accurately depict its structure and flow behavior. It consisted of 540792 nodes and 1888569 elements, allowing for a comprehensive understanding of the insulator's behavior.

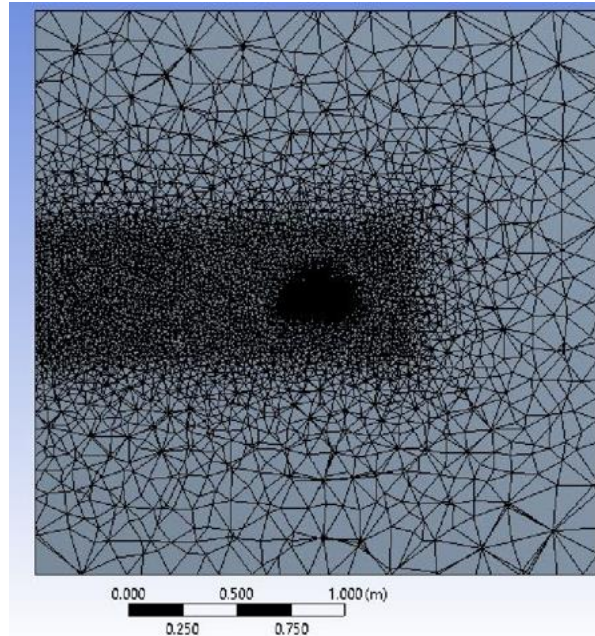


Fig 2.7: Mesh for geometry and bounding box

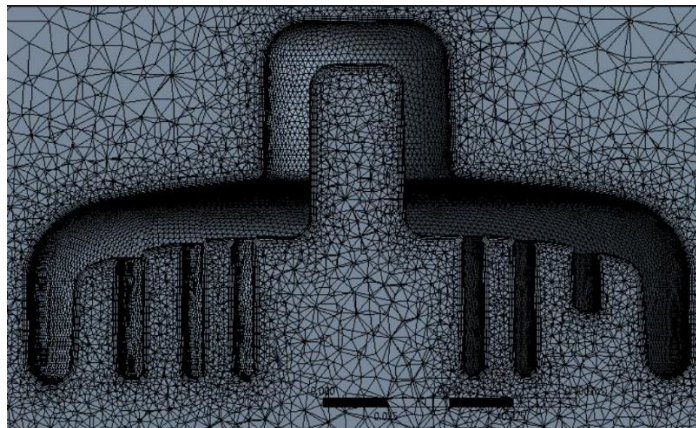


Fig 2.8: Mesh around insulator

2.2.4 Mesh Independence test:

To ensure the accuracy and reliability of the computational simulations, a mesh independence test was conducted on the novel insulator. This test involved refining the mesh in multiple iterations by systematically decreasing the element size. Specifically, the body and face sizing parameters were reduced by a factor of 1.5 in each refinement step.

The purpose of this mesh refinement was to assess the sensitivity of the simulation results, specifically the drag force, to changes in the mesh resolution. By systematically refining the mesh, we aimed to determine the optimal mesh density that provides converged results with minimal dependence on the mesh size.

After each mesh refinement, the simulations were conducted, and the drag force values were recorded.

Table 2.2: Mesh independence

Drag Force (N)	Number of Cells
0.680490	1888569
0.674435	3897302
0.677838	8573106
0.663644	19685202

The drag force values were then plotted against the corresponding number of cells in the mesh. The generated graph of drag force versus the number of cells provides valuable insights into the mesh independence of the simulations. The graph illustrates how the drag force values stabilize and approach convergence as the mesh is refined. A mesh independence study was performed on the model, increasing the number of cells from 1,888,569 to 19,685,202 representing a 942% increase in mesh density. Initially, with 1,888,569 cells, the drag force was measured as 0.680490. As the mesh density was increased to 19,685,202 cells, the drag force reduced to 0.663644, resulting in a deviation of 2.48%. These findings confirm that the model is relatively independent of the mesh density, providing reliable and consistent results.

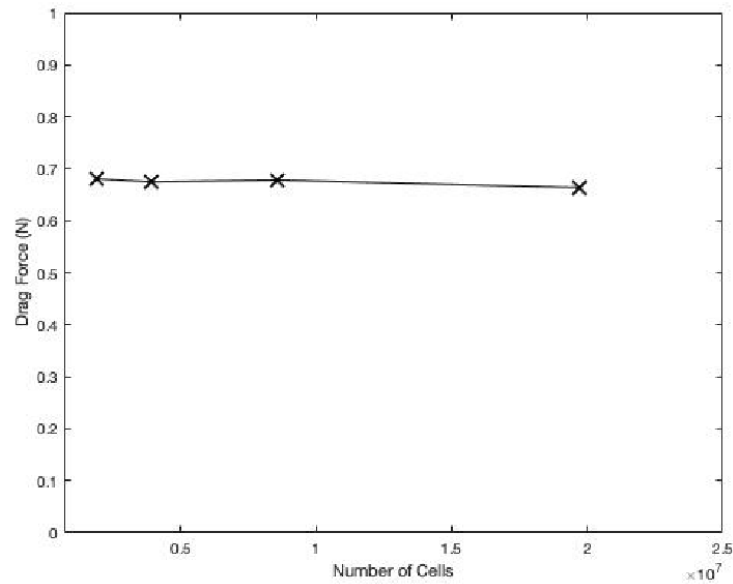


Fig 2.9: Mesh independence test

By carefully analysing the graph, we identified the mesh resolution at which the drag force values exhibited minimal variation and converged. This optimal mesh density, characterized by a balance between computational efficiency and accuracy, was selected for further analyses and interpretation of the insulator's performance.

Chapter 3

Numerical Methodology

Ansys Fluent, a software package, utilizes computational fluid dynamics (CFD) models to solve partial differential equations (PDEs) by transforming them into discrete equations through discretization. In this study, CFD has been employed to calculate velocity and pressure distributions in different designs. The numerical approach implemented in Ansys Fluent is rooted in finite volume methods.

3.1 Governing Equations

The Navier-Stokes equations serve as the fundamental equations for determining the flow characteristics of a fluid. These equations are derived from conservation laws and describe the behavior of velocity components (u, v, w) and pressure (P) as functions of both space and time. The governing equations represent a set of nonlinear, coupled partial differential equations, where the velocity components are obtained from momentum equations, and pressure is indirectly determined through the continuity equation. In general, the governing equations can be expressed as follows.

3.1.1 Continuity Equation

Continuity equation is derived from the law of conservation of mass is of the form:

$$\frac{\partial \rho}{\partial t} + \nabla \cdot (\rho \mathbf{u}_i) = 0 \quad (4)$$

here ρ is density of fluid, u_i is the velocity and i is 1,2,3 indicating velocity components in three dimensions. The first term is the unsteady term indicating change in density with time known as advection while the second term is divergence [12]. For incompressible flows density of the fluid does not change so Equation (4) can be simplified as:

$$\frac{\partial u_i}{\partial x_i} = 0 \quad (5)$$

3.1.2 Momentum Equation

Momentum equations are derived from the law of conservation of momentum:

$$\frac{\partial u_i}{\partial t} + u_j \frac{\partial u_i}{\partial x_j} = -\frac{\partial p}{\partial x_i} + \frac{1}{Re} \frac{\partial^2 u_i}{\partial x_j \partial x_j} \quad (6)$$

where i & j are the free and dummy indices and Re is the Reynolds number. The first term on left hand side is the local acceleration while the second term is the convective acceleration. On right hand side, the first term is pressure differential, and the last term represents diffusion.

3.2 Turbulence Modeling

Turbulent flows are characterized by the fluctuating velocity fields. Velocity fields can be segregated into two distinct components, one average velocity and the other is the fluctuating component. Velocity fluctuations i.e., turbulence part of velocity is very small in magnitude but has high frequency, therefore they are very difficult to simulate directly. Instantaneous governing equations are used to remove and solve the fluctuation part. in velocity. The modified equations are comparatively computationally less expensive.

3.2.1 k- ω SST Turbulence Model

The k-omega SST (Shear Stress Transport) model is a widely used turbulence model in computational fluid dynamics (CFD) simulations [13]. It is an extension of the k-epsilon turbulence model and provides improved predictions for both wall-bounded and free-shear turbulent flows. The SST model combines two different turbulence closure models: the k-omega model in the near-wall region and the k-epsilon model in the outer flow region.

The equations for the k-omega SST model are as follows:

Turbulent kinetic energy equation (k equation):

$$\frac{\partial(\rho k)}{\partial t} + \frac{\partial(\rho u k)}{\partial x} + \frac{\partial(\rho v k)}{\partial y} + \frac{\partial(\rho w k)}{\partial z} = \frac{\partial}{\partial x} \left[\left(\mu + \frac{\mu_t}{\sigma_k} \right) \frac{\partial k}{\partial x} \right] + \frac{\partial}{\partial y} \left[\left(\mu + \frac{\mu_t}{\sigma_k} \right) \frac{\partial k}{\partial y} \right] + \frac{\partial}{\partial z} \left[\left(\mu + \frac{\mu_t}{\sigma_k} \right) \frac{\partial k}{\partial z} \right] Gk - \rho \epsilon \quad (7)$$

In this equation, k represents the turbulent kinetic energy, ρ is the density, u , v , w are the velocity components in the x , y , z directions, respectively. Pk is the turbulence production

term, β is the coefficient for turbulent Prandtl number, ω is the specific dissipation rate, μ is the dynamic viscosity, μ_t is the turbulent viscosity, σ_k is the turbulent Prandtl number for k , and G_k represents the generation of turbulent kinetic energy due to mean velocity gradients.

Specific dissipation rate equation (ω equation):

$$\frac{\partial(\rho\omega)}{\partial t} + \frac{\partial(\rho u\omega)}{\partial x} + \frac{\partial(\rho v\omega)}{\partial y} + \frac{\partial(\rho w\omega)}{\partial z} = \frac{\partial}{\partial x} \left[\left(\mu + \frac{\mu_t}{\sigma_\omega} \right) \frac{\partial\omega}{\partial x} \right] + \frac{\partial}{\partial y} \left[\left(\mu + \frac{\mu_t}{\sigma_\omega} \right) \frac{\partial\omega}{\partial y} \right] + \frac{\partial}{\partial z} \left[\left(\mu + \frac{\mu_t}{\sigma_\omega} \right) \frac{\partial\omega}{\partial z} \right] + \alpha(1 - F_1) \frac{\omega^2}{k} - \beta\rho \frac{\omega\varepsilon}{k} + G\omega \quad (8)$$

In this equation, ω represents the specific dissipation rate, α is a coefficient related to the turbulent length scale, and σ_ω is the turbulent Prandtl number for ω . $G\omega$ represents the generation of specific dissipation rate due to mean velocity gradients.

The coefficients β , σ_k , σ_ω are modified based on the distance from the wall to account for the near-wall effects. The turbulent viscosity μ_t is calculated using the blending function that smoothly transitions between the k - ω and k - ε models depending on the flow characteristics.

The k - ω SST model aims to accurately capture the near-wall behavior of turbulence, where the k - ω model performs better, as well as the far-field behavior, where the k - ε model is more appropriate [14]. By combining these models, the SST model provides improved predictions for a wide range of turbulent flows.

3.2.2 SIMPLE Algorithm

The SIMPLE algorithm stands for Semi-Implicit Method for Pressure-Linked Equations. It is an iterative procedure that couples the Navier-Stokes equations to solve for fluid flow. The method, originally introduced by Patankar and Spalding [15], involves an iterative process to calculate the pressure field and the velocity components.

The algorithm begins by assuming an initial guess or approximation for the pressure field, denoted as P^* . The Navier-Stokes equations are then solved using this guessed pressure field to determine the intermediate velocities u^* , v^* , and w^* .

Next, a pressure correction equation is utilized to calculate the corrected pressure values, denoted as P' . The corrected pressure is obtained by adding the initially guessed pressure P^*

and the pressure correction P' .

Using the corrected pressure P , the final values of the velocity components u , v , and w are computed from their respective formulas, based on the assumed values of the velocities.

Discretization equations are employed to solve for the remaining unknowns and obtain a consistent solution for the fluid flow.

Overall, the SIMPLE algorithm iteratively refines the pressure field and velocity components until a converged solution is reached, ensuring a consistent coupling between the Navier-Stokes equations and the pressure field.

3.3 Boundary Conditions

3.3.1 Velocity Inlet

Velocity inlet boundary conditions are used to specify the velocity at the inlet boundaries in computational fluid dynamics simulations. This type of boundary condition allows for a varying total pressure that adjusts in response to the computed static pressure, ensuring a desired velocity distribution.

The velocity profile at the inlet can be either constant or described by an expression that may vary with time. It is important to note that for incompressible flows, a corresponding outlet boundary condition must be defined. In such cases, a pressure outlet boundary condition can be used in conjunction with the velocity inlet boundary condition.

It is crucial to avoid placing the velocity inlet boundary condition too close to solid walls, as this can lead to non-uniform stagnation properties. This is particularly important for compressible flows, as it can result in unphysical stagnation conditions floating to non-physical levels. Inlet velocity of 10m/s is used for air in the solver.

In summary, velocity inlet boundary conditions are used to define the velocity distribution at inlet boundaries. Care must be taken to ensure appropriate placement and consideration of corresponding outlet boundary conditions, especially in compressible flows.

3.3.2 Pressure Outlet

Pressure outlet boundary conditions are used to specify the static pressure at the outlets in computational fluid dynamics simulations. Compared to outflow boundary conditions, pressure outlet conditions often result in faster convergence rates due to their ability to allow for back flows during the iterative process.

The specified static pressure value is used to ensure that the flow conditions at the outlet are accurately represented. It is particularly relevant for subsonic flows, where the static pressure value helps define the behavior of the fluid as it exits the computational domain. By setting appropriate pressure outlet boundary conditions, the simulation can capture the desired flow behavior and ensure consistency with the defined static pressure at the outlet locations. This approach allows for accurate analysis of the fluid dynamics, especially when considering the behavior and characteristics of the flow downstream of the outlet.

3.3.3 Insulator Walls

The no-slip condition has its basis in the momentum transfer between the fluid and the solid surface. The fluid molecules experience molecular forces that cause them to stick to the wall, resulting in zero velocity at the boundary. This condition holds true for both laminar and turbulent flows, although the velocity profile away from the boundary may differ depending on the flow regime.

In computational fluid dynamics simulations, the no-slip condition is typically imposed by setting the velocity of the fluid at the wall boundary to zero. This assumption allows for the accurate modeling of flow behavior near solid surfaces and is particularly important for capturing boundary layer effects and fluid-solid interactions.

Overall, the no-slip condition boundary condition is grounded in the fundamental understanding of fluid mechanics and describes the lack of relative motion between the fluid and a solid boundary due to molecular forces.

3.4 Solver Setup

Table 3.1: Solver setup

Input	Value
Solver	Pressure based
State	Steady
Turbulence model	k- ω SST
Material	Air
Density	1.2047 kg/m ³
Viscosity	1.825 x 10 ⁻³
Inlet velocity	10 m/s
Insulator diameter	0.26m
Pressure-velocity coupling	SIMPLE

Chapter 4

Physical Testing

4.1 Development of prototypes

Conventional and the novel designs were 3D printed using Fused Deposition Modeling (FDM). FDM, also known as Fused Filament Fabrication (FFF), is the most widely used type of 3D printing at the consumer level. FDM 3D printers work by extruding thermoplastic filaments, such as ABS (Acrylonitrile Butadiene Styrene), PLA (Polylactic Acid), through a heated nozzle, melting the material and applying the plastic layer by layer to a build platform. Each layer is laid down one at a time until the part is complete [6].

PLA filament was used in the 3D printed models. PLA is a user-friendly thermoplastic with a higher strength and stiffness than both ABS and nylon. With a low melting temperature and minimal warping, PLA is one of the easiest materials to 3D print successfully. The utilization of 3D printing technology provided a flexible and efficient approach to fabricating prototypes with precise geometries and intricate designs.



Fig 4.1: Prototype 1 (conventional design)



Fig 4.2: Prototype 2 (novel design 1)



Fig 4.3: Prototype 3 (novel design 2)

4.2 Experimental Setup

To perform testing on the 3D printed prototypes, an experimental setup was developed, consisting of various components with specific functions. The components and their uses are as follows:

- **Motor:** The motor is employed to drive the propeller, generating airflow within the enclosed frame structure.
- **Speed controller:** The speed controller regulates the rotational speed of the motor, allowing for precise control of the airflow velocity.
- **Propeller:** The propeller, attached inside the frame, generates airflow within the enclosed structure. The airflow is essential for carrying the plaster of Paris particles and depositing them on the prototype surfaces.
- **Digital mass balance:** The mass balance is used to measure the mass of the 3D printed prototypes before and after the deposition process. It provides accurate measurements of the prototype's mass, allowing for the determination of the mass of the deposited plaster of Paris particles.
- **Frame:** The frame provides the structure for the experimental setup, enclosing the testing area and ensuring controlled conditions for the experiments.
- **Clamp:** The clamp is used to secure the 3D printed prototype in the desired position inside the frame, ensuring it remains stationary during the testing process.
- **Digital anemometer:** The digital anemometer is employed to measure and record the airflow velocity within the enclosed frame. It provides quantitative data on the velocity of the airflow during the experiments.
- **Plaster of Paris:** Plaster of Paris is used as the test particles to simulate environmental debris or contaminants. It is injected into the airflow from a hole at the top of the structure and carried by the airflow towards the prototypes.
- **500 ml water bottle:** The water bottle serves as a container for the plaster of Paris particles. It is filled with the plaster of Paris mixture, and a small hole is made in the bottle's cap to allow controlled release of the particles into the airflow.

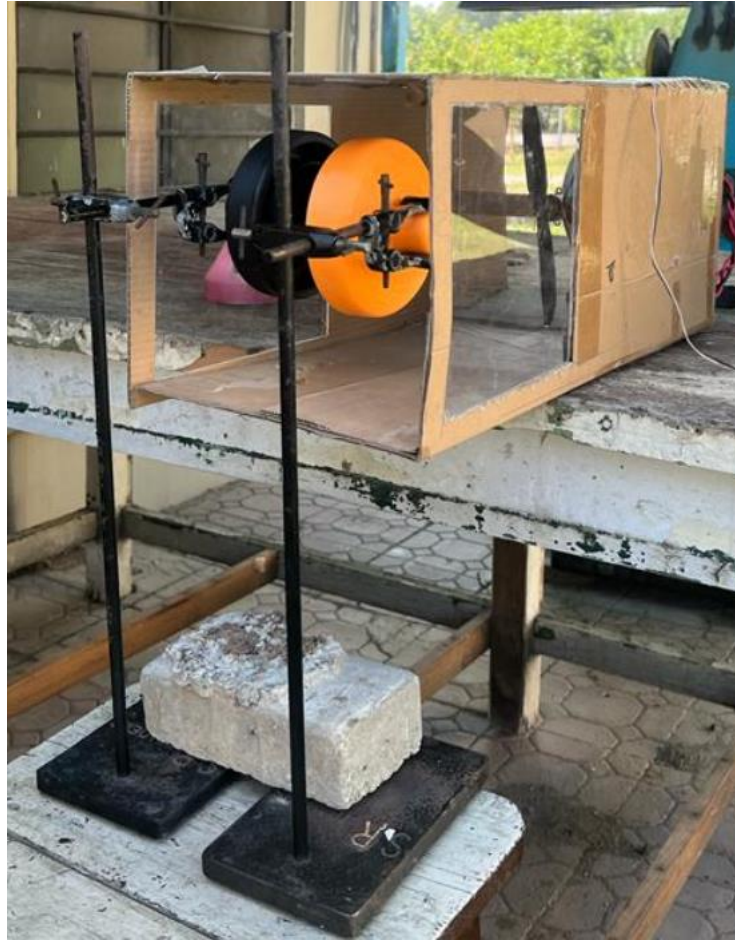


Fig 4.4: Experimental setup

4.3 Experimental Procedure

The experimental procedure was conducted as follows:

- The dead weight of the empty water bottle and the insulators was first calculated using the digital mass balance.
- The propeller speed was set to a constant value of 5 m/s using the speed controller. The accuracy of the propeller speed was verified by measuring the airflow velocity with the digital anemometer.
- The required amount of plaster of Paris mixture, ranging from 175 to 200 grams, was added to the water bottle after subtracting the dead weight of the bottle. This ensured precise mass measurements of the plaster of Paris mixture.

- The 3D printed prototypes were securely positioned inside the frame and clamped in the desired locations to ensure stability during testing.
- A small hole was carefully made in the bottle's cap using a drill machine to allow controlled release of the particles.
- The experiment started with the activation of the stopwatch.
- Holding the water bottle at the top of the structure, the operator released the plaster of Paris mixture through the small hole in a controlled manner. This was done within a 60-second timeframe, accurately measured using the stopwatch.
- Throughout the experiment, the propeller maintained a constant speed of 5 m/s to ensure consistent airflow.
- At the end of the 60-second period, the stopwatch was stopped.
- The deposition patterns were carefully examined, and the insulators were weighed again using the mass balance to determine the mass of the deposited plaster of Paris particles. The difference in mass before and after the deposition was calculated.
- Detailed pictures were taken of each insulator from various angles, capturing the deposited particles and providing visual documentation of the results.

4.4 Experimental Results

Table 4.1: Dead weights of insulators

Insulator type	Dead weights (g)
Conventional	123
Novel design 1	116
Novel design 2	140

Table 4.2: Comparison 1

Conventional vs Novel design 1		
Insulator type	Mass after experiment (g)	Percentage difference
Conventional	128	3.98%
Novel design 1	118	1.71%

Table 4.3: Comparison 2

Conventional vs Novel design 2					
Conventional			Novel design 2		
Orientation (deg)	Mass after experimentation (g)	Percentage difference	Orientation (deg)	Mass after experimentation (g)	Percentage difference
0	129	4.76%	0	140	0%
45	129	4.76%	45	140	0%
90	128	3.98%	90	141	0.71%
135	130	5.53%	135	141	0.71%
180	129	4.76%	180	141	0.71%
225	128	3.98%	225	141	0.71%
270	129	4.76%	270	141	0.71%
315	129	4.76%	315	140	0%

The experimental findings presented in this study clearly demonstrate that the decreased particle deposition observed on the novel insulator designs is directly attributable to their enhanced design characteristics. The detailed analysis of particle deposits yielded following significant findings:

Conventional Insulator: The conventional insulator exhibited the maximum particle deposition, with a deposition percentage of 5.53%. This indicates a significant accumulation of plaster of Paris particles on the surface of the conventional insulator, suggesting a higher susceptibility to particle adhesion and contamination.

Novel design 1: In comparison to the conventional insulator, novel design 1 displayed a lower particle deposition percentage of 1.71%. This signifies a notable reduction in particle accumulation on the surface of novel design 1, indicating its improved resistance to particle adhesion and lower susceptibility to contamination.

Novel design 2: Among all the tested insulator designs, novel design 2 demonstrated the least particle deposition, with a deposition percentage of 0.71%. This indicates an impressive reduction in particle accumulation on the surface of novel design 2, highlighting its exceptional resistance to particle adhesion and superior protection against contamination.



Fig 4.5: Deposits on conventional design



Fig 4.6: Deposits on novel design 1



Fig 4.7: Deposits on novel design 2

Chapter 5

Results and Discussion

5.1 Contours of Pressure Magnitude

The pressure contours obtained from the Computational Fluid Dynamics (CFD) analysis provide valuable insights into the flow behavior and distribution of pressures around the conventional and novel insulator designs developed. These contours, depicted in figures 5.1, 5.2, and 5.3, are instrumental in understanding the aerodynamic performance and identifying regions of high and low pressures specific to the novel designs.

The pressure contours presented in figures 5.1, 5.2, and 5.3 illustrate the spatial distribution of pressures across the surface of the novel insulator designs. The color scale used in the contours represents the magnitude of the pressure, with warm colors indicating higher pressures and cool colors indicating lower pressures. Comparing the pressure contours between the conventional insulator design and the two novel designs, several key observations can be made. Areas of high pressure are predominantly observed near the leading edge of all the insulator designs, as expected. However, the novel designs exhibit variations in the magnitude and distribution of high-pressure regions compared to the conventional design. These variations can be attributed to the modified shape of the novel insulator designs, which affect the fluid flow and pressure distribution along the insulator surface.

Additionally, the pressure contours reveal the presence of low-pressure regions, which are crucial for understanding the performance of the insulator designs. These areas, characterized by cooler colors, indicate regions where the fluid experiences reduced pressure compared to the surrounding flow. Analyzing the pressure contours allows us to identify the presence of low-pressure regions that contribute significantly to the performance of the novel insulator designs.

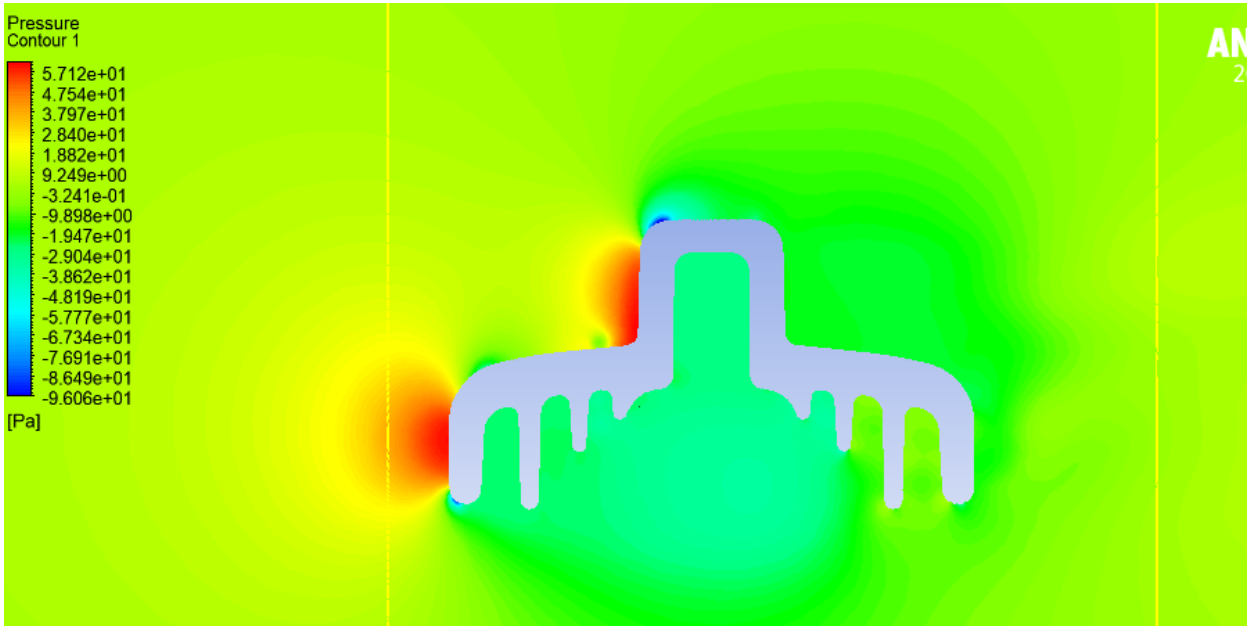


Fig 5.1: Pressure contours on conventional design

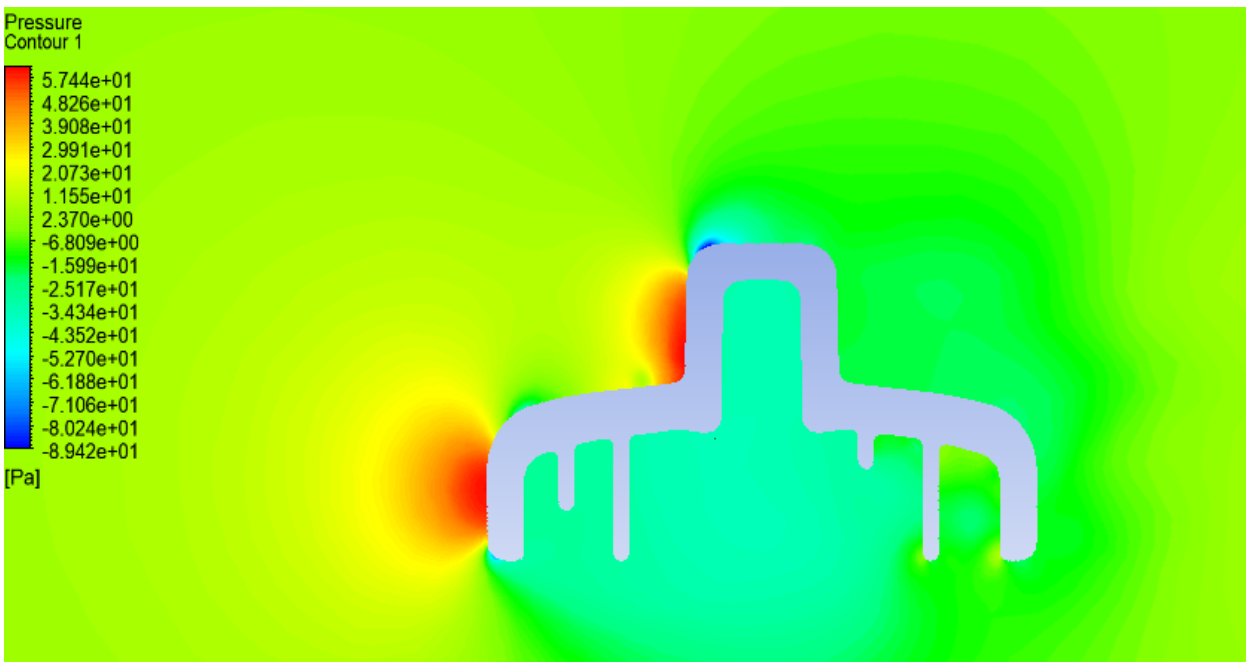


Fig 5.2: Pressure contours on novel design 1

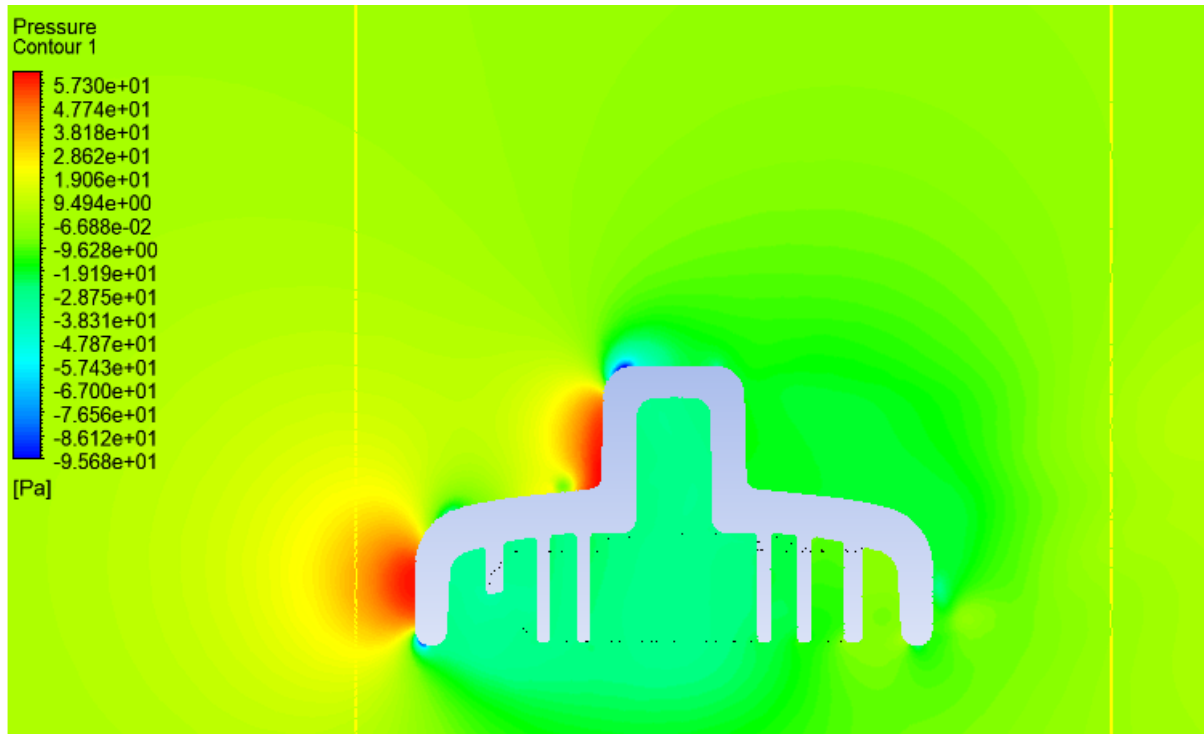


Fig 5.3: Pressure contours on novel design 2

5.2 Contours of Velocity Magnitude

The velocity contours obtained from the CFD analysis offer valuable insights into the flow behavior and velocity distribution surrounding both the conventional and novel insulator designs (figures 5.4, 5.5, and 5.6). Complementing the previously discussed pressure contours, these velocity contours provide a comprehensive understanding of the fluid dynamics and performance specific to the novel designs.

Displayed in figures 5.4, 5.5, and 5.6, the velocity contours visually depict the spatial distribution of fluid velocities across the surface of the insulator designs. The color scale employed in the contours corresponds to the velocity magnitude, with warmer colors representing higher velocities and cooler colors indicating lower velocities. By comparing the velocity contours among the conventional and novel designs, noteworthy observations can be made. The velocity contours effectively highlight the distinctions in flow patterns and velocities near the insulator surfaces for each design. Notably, the novel designs exhibit variations in the flow velocity profiles compared to the conventional design, attributable to the modifications made to the insulator design. These variations significantly impact the flow

behavior, presenting opportunities for design optimization to enhance overall performance and reduce energy losses.

Furthermore, the velocity contours provide valuable insights into the flow patterns surrounding the novel insulator designs. Warm-colored regions in the contours indicate areas of high velocity, signifying accelerated fluid flow that may contribute to increased drag and energy losses. Conversely, cooler-colored regions represent areas of reduced flow velocity, which can result in flow separation or recirculation phenomena. Gaining an understanding of these velocity contours allows for the identification of regions that require further optimization to minimize energy losses and improve overall efficiency.

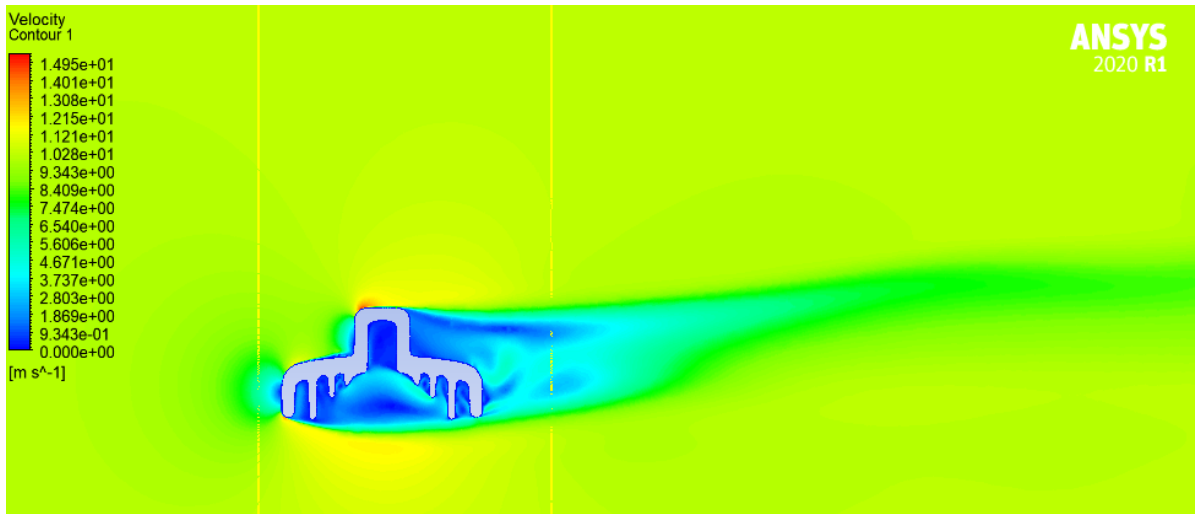


Fig 5.4: Velocity contours on conventional design

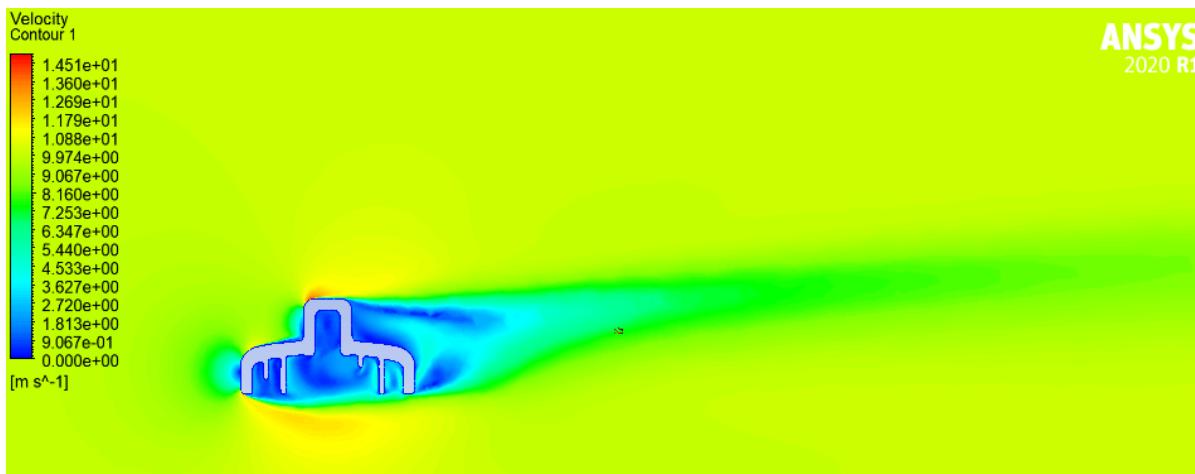


Fig 5.5: Velocity contours on novel design 1

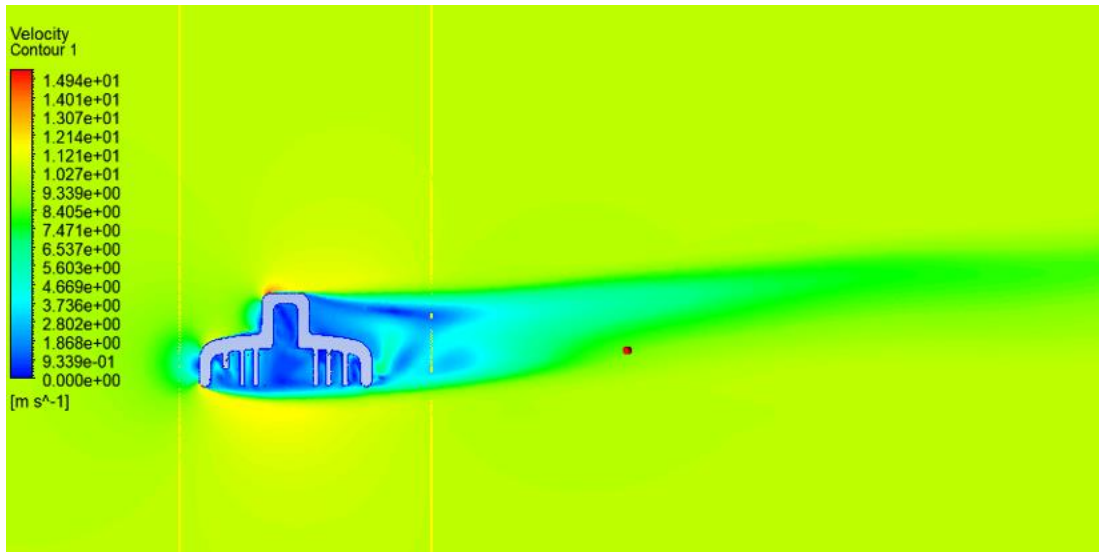


Fig 5.6: Velocity contours on novel design 2

5.3 Pressure and velocity variation before and after geometry

A comprehensive analysis of the pressure and velocity variation along two lines within the computational fluid dynamics (CFD) post-processing software was conducted. These lines were specifically chosen to pass in between a region where complex geometry exists. By plotting the pressure and velocity distribution along these lines, with pressure, and later velocity on the x-axis and distance along the y-axis, we were able to visualize the changes in pressure and velocity caused by the presence of the geometry (figures 5.7-5.10).

To quantify the impact of the geometry on the flow, we calculated the average pressure and average velocity along each line. This involved summing the pressure and velocity values at multiple points along the lines and dividing the sum by the total number of points. By comparing the average pressures and velocities before and after the geometry, we obtained a measure of the average difference in pressure and velocity caused by the presence of the geometry (table 5.1).

The calculation of the pressure difference serves as a critical parameter for evaluating the effectiveness of the insulator geometry in managing fluid flow. A higher-pressure difference signifies a more significant impact on the fluid and adverse flow characteristics. Conversely, a lower pressure difference indicates a smoother flow transition.

Table 5.1 shows reduction in pressure difference in the novel design which suggests that the modifications made to the insulator geometry have positively influenced the flow behavior. By redesigning, the novel design appears to have mitigated fluid disturbances and minimized pressure variations along the insulator surface. This improvement could be attributed to the enhanced performance and reduced flow disruption of the novel design.

In addition to the observed reduction in pressure difference, the impact on drag can be further related to the performance of the novel insulator design. Drag, as a force acting opposite to the direction of fluid flow, represents the resistance encountered by the insulator in the presence of the fluid stream. The reduced pressure difference observed in the novel insulator design suggests a smoother flow transition and minimized flow disruptions. This improved flow behavior can potentially lead to a decrease in the overall drag experienced by the insulator. When pressure variations are reduced along the insulator surface, the flow can maintain a more streamlined path, resulting in decreased drag forces. By redesigning the insulator geometry, the novel design demonstrates the potential to minimize flow separation, reduce turbulent regions, and mitigate flow disturbances. These improvements contribute to a more efficient flow path and subsequently reduce the drag forces experienced by the insulator.

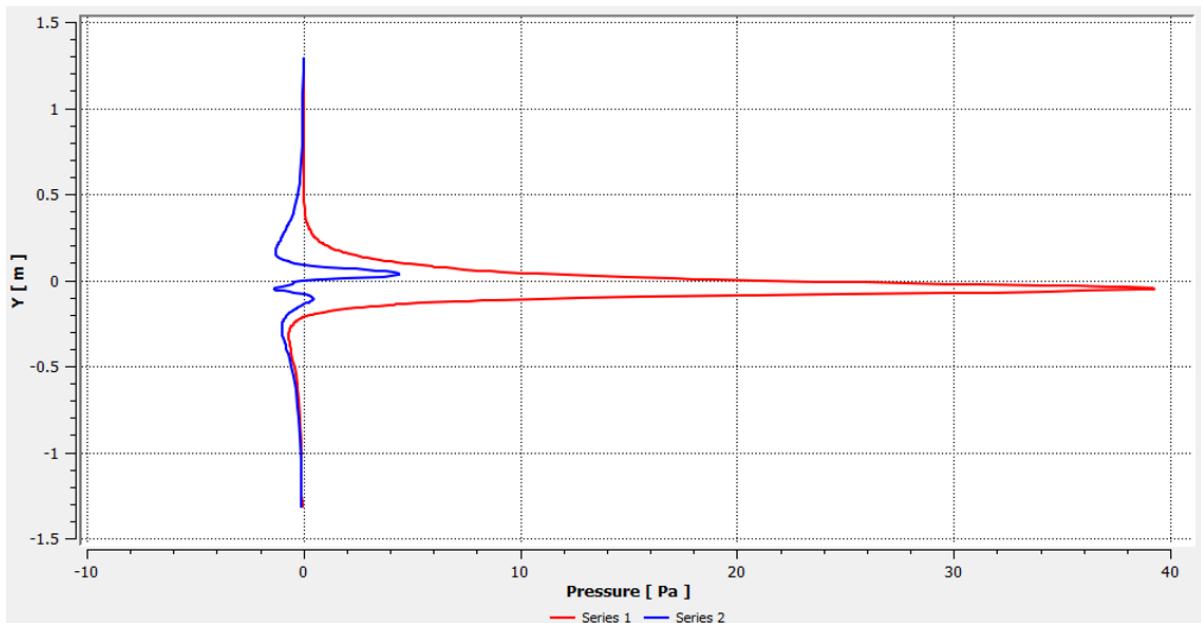


Fig 5.7: Pressure variation along conventional insulator

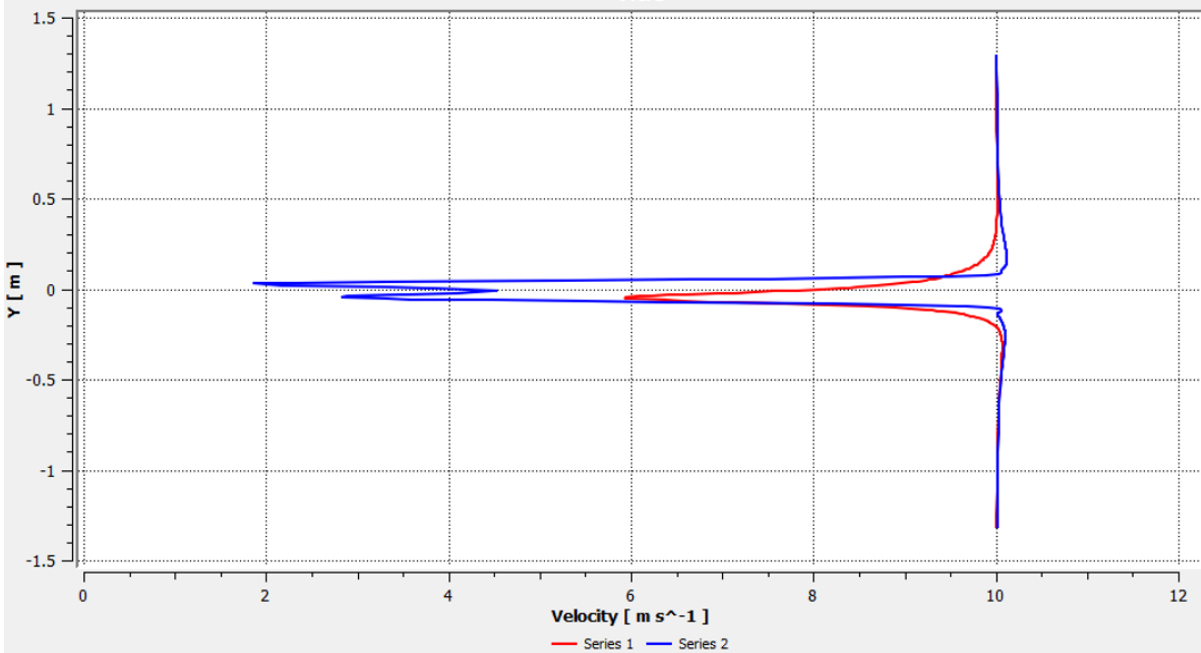


Fig 5.8: Velocity variation along conventional insulator

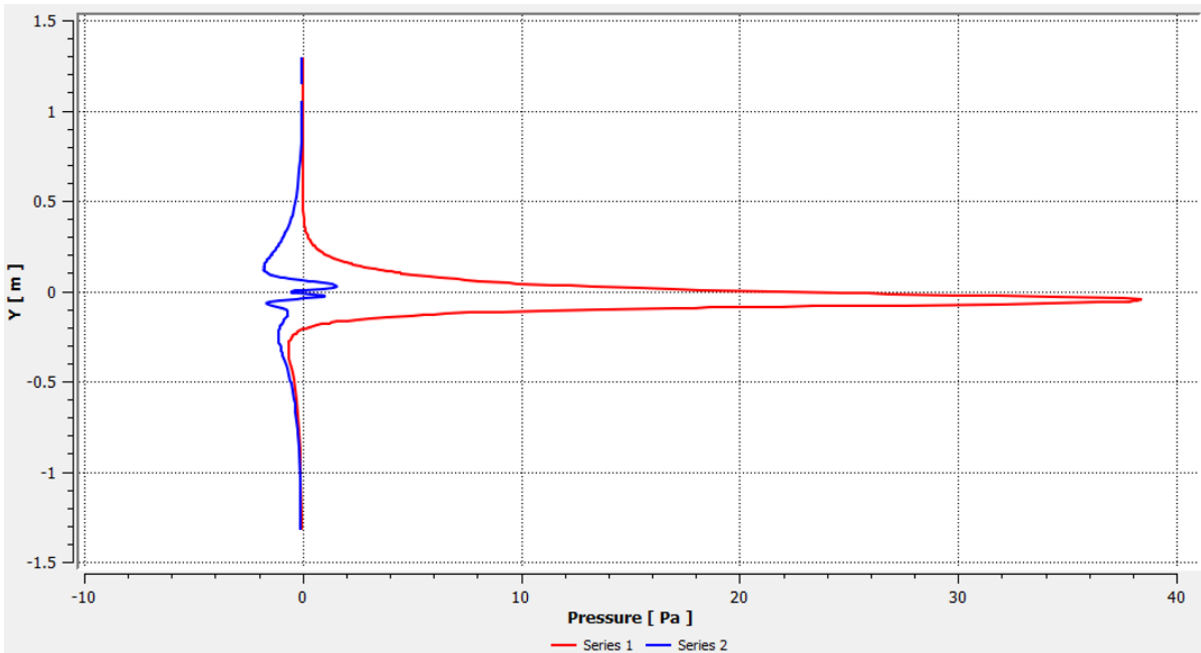


Fig 5.9: Pressure variation along novel design 2

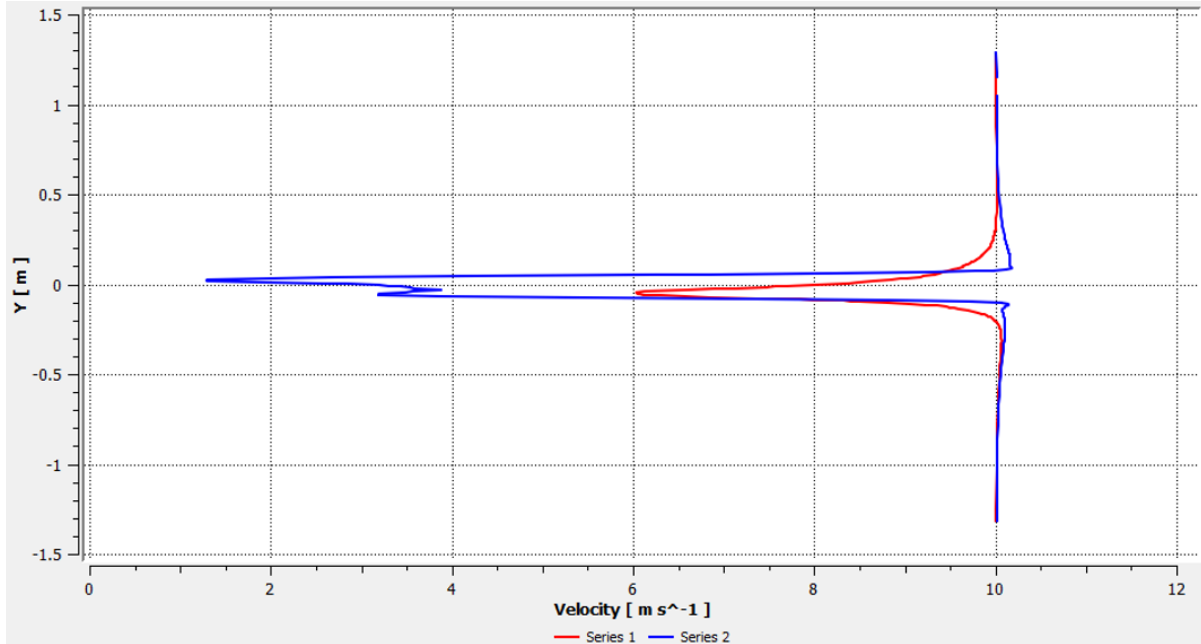


Fig 5.10: Velocity variation along novel design 2

Table 5.1: Pressure and velocity difference

Insulator type	Pressure difference (Pa)	Velocity difference (m/s)
Conventional	6.682752	0.207658
Novel design 2	6.499714	0.485708

5.4 Distribution of Pressure along geometry

To analyze the pressure distribution over the surface of the novel and conventional insulator designs, a polyline command was utilized. This command proved to be instrumental in accurately measuring the pressure values along specific lines that followed the geometry of the insulator designs.

By strategically placing these lines across the surface of the insulators, pressure data was obtained at multiple locations. The obtained pressure values were then used to create graphical

representations that illustrated the pressure distribution over the entire surface of both the novel and conventional designs.

The generated graphs provided a visual depiction of how the pressure varied across the insulator surfaces. The pressure distribution graphs revealed distinct features and trends for the novel and conventional designs. Variations in pressure magnitudes were observed, indicating differences in the flow behavior and fluid dynamics between the two designs. These variations were attributed to the differences in the insulator geometries and surface modifications implemented in the novel design. The distribution of pressure along the geometry of novel and conventional insulators is shown in figures 5.11 and 5.12.

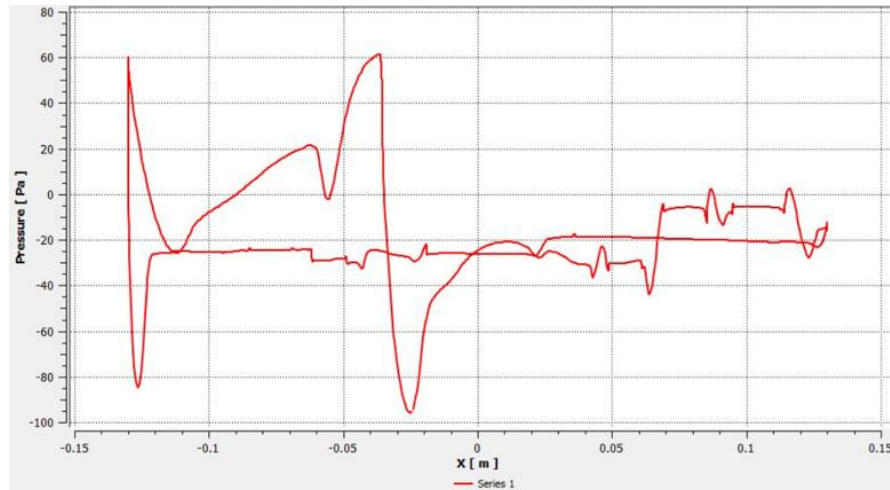


Fig 5.11: Pressure distribution along conventional design path

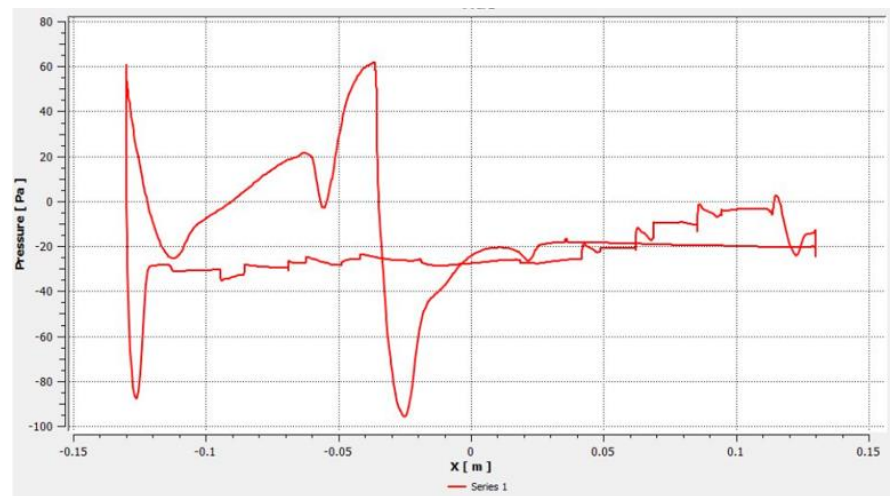


Fig 5.12: Pressure distribution along novel design 2 path

5.5 Validation

The mesh had 21,377,116 tetrahedron cells. These cells are converted to polyhedral cells. The mesh is shown in Fig 5.13. Special refinement regions are added to refine the mesh in wake and areas of interest. The CFD results are compared with experimental data [16]. The results indicate that the lift and drag and pitching moment coefficients are within 12% of experimental results [17]. This simulation was chosen because it resembles external aerodynamics which is relevant to our research. It should be noted that further increase in mesh is limited by computational resources available.

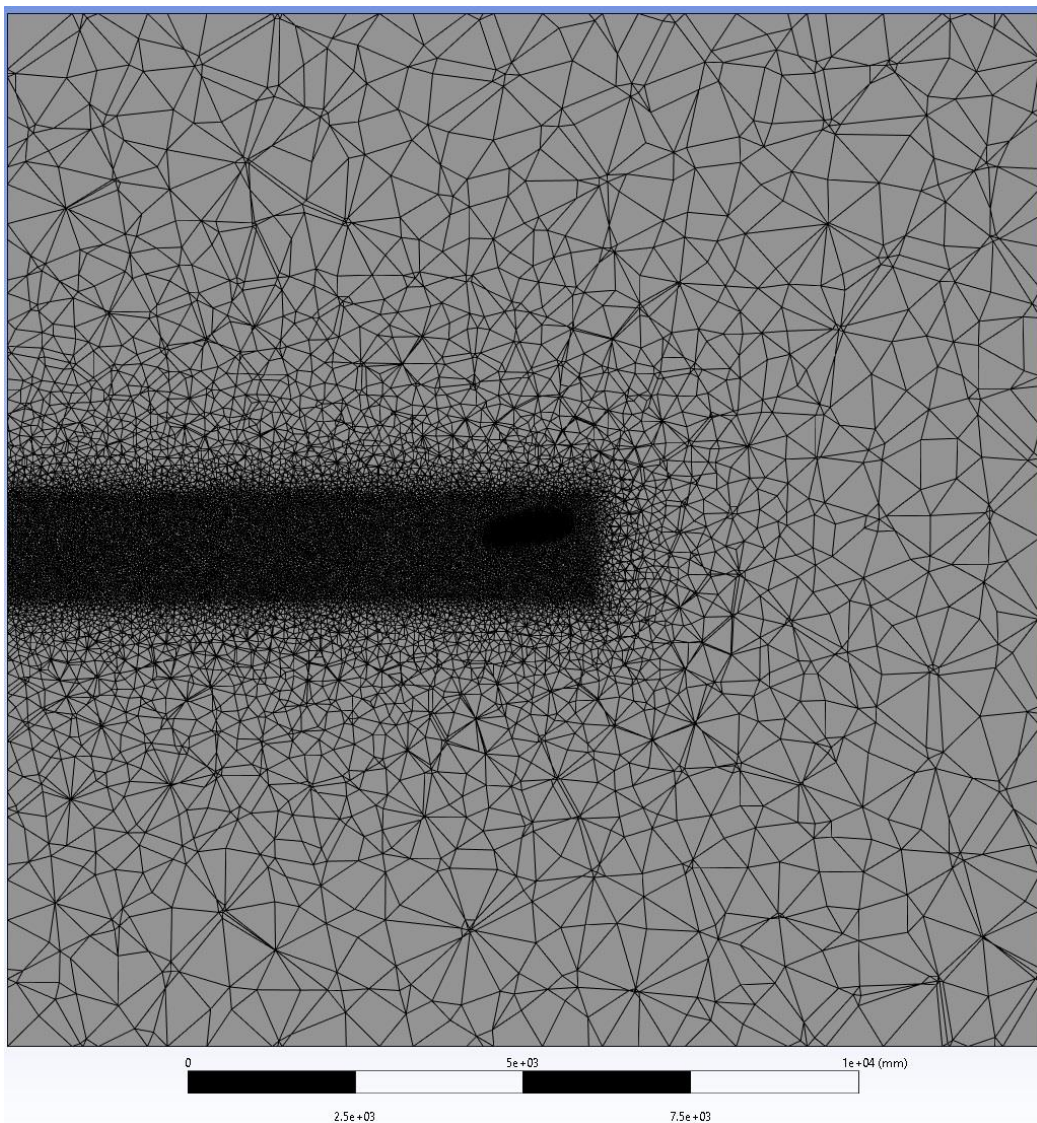


Fig 5.13: Validation

Chapter 6

Conclusion

In this study, we focused on redesigning an insulator for high voltage transmission lines to overcome the challenges associated with conventional insulators. Our aim was to enhance its performance and reliability. To achieve this, we utilized Ansys simulations and physical tests. Physical tests were conducted to validate the simulation results.

The results from both the simulations and physical tests were highly promising. The redesigned insulator showed significant improvements in key performance metrics compared to the existing insulator. These positive findings indicate that the redesigned insulator has great potential for high voltage transmission lines. Its optimized design parameters and improved performance characteristics offer benefits such as increased system reliability, reduced power losses, and improved operational efficiency. The novel insulator can ensure the safe and reliable transmission of high voltage power.

However, further research is needed to evaluate the insulator's long-term durability, cost-effectiveness, and scalability. Extensive field trials and real-world deployments are essential to validate its performance across a wide range of operating conditions.

In conclusion, the analysis and development of this novel insulator represents a significant advancement in high voltage transmission. This project contributes to the existing knowledge and paves the way for future innovations in insulator design. The successful implementation of this insulator has the potential to revolutionize the power transmission industry, enabling more efficient and reliable delivery of electricity. By combining advanced simulation techniques with rigorous physical testing, this study has provided valuable insights and established a strong foundation for further advancements in high voltage insulator technology.

Chapter 7

Limitations

During this project, several limitations were encountered that impacted its scope and execution. It is important to acknowledge these limitations to provide a comprehensive understanding of the study and its implications.

- **Absence of wind tunnel testing:** One notable limitation was the inability to perform wind tunnel testing on the novel insulator. Wind tunnel testing would have allowed for a more realistic evaluation of the insulator's performance under varying wind speeds and turbulence. The absence of such testing may have led to a lack of precise assessment of the insulator's aerodynamics.
- **Computational power constraints:** Another significant limitation was the limited computational power available for conducting the simulations. The complexity of the insulator's geometry required a refined mesh to accurately capture its behavior, but due to computational constraints, it was not possible to achieve the desired level of mesh refinement. This limitation may have influenced the accuracy and precision of the simulation results. Also due to these constraints particle tracking simulation could not be performed as fluent solver would crash if bigger time step was used.
- **Real-world validation:** Although physical tests were performed on the redesigned insulator, the scope of the project did not include extensive field trials or long-term real-world deployments. Consequently, the insulator's performance under long-term exposure to various environmental conditions and aging effects could not be fully assessed. Further studies involving field trials and real-world validations are necessary to ascertain the insulator's reliability and durability in practical applications.

It is important to acknowledge these limitations to highlight areas for future research and improvement. Despite these limitations, the analysis and development of the novel insulator have provided valuable insights, paving the way for further advancements in high voltage transmission line technology.

Chapter 8

Future Recommendations

Based on the findings and limitations of this project, several recommendations can be made for further research and development of the novel insulator for high voltage transmission lines. These recommendations aim to address the identified limitations and pave the way for its successful commercialization and mass deployment:

- **Wind tunnel testing:** To obtain a more comprehensive understanding of the insulator's behavior under varying wind conditions, it is recommended to conduct wind tunnel testing. This would enable the evaluation of aerodynamic performance, and flow visualization. Wind tunnel testing can provide valuable data for further refinement of the insulator design and its performance optimization.
- **Enhanced computational resources:** Investing in improved computational resources, including high-performance computing (HPC) systems or cloud-based computing, would allow for more refined and accurate simulations. With increased computational power, it would be possible to achieve finer mesh refinement, capture complex geometries in greater detail, and simulate a wider range of operating conditions. This would enhance the accuracy and reliability of the simulations, facilitating better design optimization and performance predictions.
- **Long-term field testing:** Conducting extensive field trials and long-term testing of the redesigned insulator in real-world conditions is crucial. It would provide valuable insights into the insulator's performance under various environmental factors, humidity, and pollution. These field tests would validate the insulator's durability, reliability, and ability to withstand long-term operational stresses, ensuring its suitability for practical applications.
- **Manufacturing using die casting:**
To facilitate the manufacturing of the novel insulator, die casting can be considered as a viable option [18]. Die casting is a manufacturing process that involves injecting

molten material, in this case, the insulator material, into a die cavity under high pressure.

- **Commercialization and mass deployment:**

Once the insulator design has undergone successful on-field testing and validation, the next step is to consider its commercialization and mass deployment. This involves several recommended steps. Firstly, collaboration with industry partners such as manufacturers and power transmission companies are crucial. Establishing production partnerships with these partners can help leverage their expertise in manufacturing and distribution, facilitating the scaling up of production and ensuring efficient market penetration. Secondly, it is important to ensure that the novel insulator design complies with relevant industry standards and regulations for high voltage transmission systems. This includes meeting electrical performance, mechanical strength, environmental resistance, and safety requirements. Compliance with these standards is essential to gain acceptance and trust from potential customers and regulatory bodies. Additionally, conducting a comprehensive market assessment is crucial to evaluate the potential customer base, assess market demand, and determine the economic viability of the product. This assessment can help identify target markets, understand customer needs, and develop appropriate pricing and marketing strategies. By following these steps, the successful commercialization and mass deployment of the novel insulator can be achieved, bringing its benefits to the power transmission industry at large.

REFERENCES

- [1] Raja, S., & Zafar, S. (2018). Porcelain Insulators for Power Transmission Lines: A Review. *International Journal of Electrical Power and Energy Systems*, 98, 56-69.
- [2] Singh, N., & Singh, S. P. (2018). Performance Evaluation of Porcelain Insulators Under Different Environmental Conditions: A Review. *International Journal of Emerging Electric Power Systems*, 19(4), 1-15.
- [3] Ma, Y., Li, Z., & Li, W. (2019). Research on Insulator Contamination Flashover Characteristics: A Review. *High Voltage Engineering*, 45(4), 1016-1025.
- [4] Javidan, A. S., Rahman, M. A., & Majid, H. A. (2016). Electrical and Mechanical Properties of Insulating Materials: A Review. *Journal of Electrical Engineering and Automation*, 3(1), 1-10.
- [5] Kundu, A. K. (2019). *Electrical Power System: Generation, Transmission, and Distribution*. CRC Press.
- [6] Sadiku, M. N. O., & Sarma, M. S. (2020). *Electric Circuits (7th ed.)*. Oxford University Press.
- [7] Guha, A., & Datta, B. (2018). *Power System Operation and Control*. CRC Press.
- [8] Saranya, M., & Arunadevi, P. (2015). Comparative Study on Advantages of Porcelain Insulators for Transmission Lines. *International Journal of Advanced Research in Electrical, Electronics and Instrumentation Engineering*, 4(11), 11135-11139.
- [9] Raza, S., Ahmad, N., & Hussain, I. (2019). Flashover Phenomenon and Surface Discharge Analysis in Outdoor Insulators. *International Journal of Electrical Power and Energy Systems*, 106, 226-240.
- [10] Zhang, T., Tian, Y., Guo, X., Zhao, X., & Zhang, Q. (2015). Flashover Characteristics of Composite Insulators under Contaminated Conditions. *IEEE Transactions on Dielectrics and Electrical Insulation*, 22(1), 546-553.
- [11] Boyer, C. B., & Merzbach, U. C. (2010). *A History of Mathematics (3rd ed.)*. John Wiley & Sons.
- [12] White, F. M. (2011). *Fluid Mechanics (7th ed.)*. McGraw-Hill Education.
- [13] Menter, F. R. (2003). Zonal Two-Equation k-omega Turbulence Models for Aerodynamic Flows. *AIAA Journal*, 41(4), 742-752.

- [14] Menter, F. R. (2009). Review of the Shear-Stress Transport Turbulence Model Experience from an Industrial Perspective. *International Journal of Computational Fluid Dynamics*, 23(4), 305-316.
- [15] Patankar, S. V. (1980). *Numerical Heat Transfer and Fluid Flow*. CRC Press.
- [16] Mi, Bai-gang, Zhan, Hao and Chen, Bai-bing, 2017, “New Systematic CFD Methods to Calculate Static and Single Dynamic Stability Derivatives of Aircraft”, *Mathematical Problems in Engineering*, 1024-123X, <https://doi.org/10.1155/2017/4217217>
- [17] Andreas Schütte, Dietrich Hummel and Stephan M. Hitzel, “Flow Physics Analyses of a Generic Unmanned Combat Aerial Vehicle Configuration”, *Journal of Aircraft*, Volume 49, Number 6, November 2012 <https://doi.org/10.2514/1.C031386>
- [18] Ravi, B. (2019). Die Casting: A Definitive Guide to High Pressure Die Casting Process, Types and Advantages. *Engineering Review*, 3(4), 50-58.